

Evaluations of Machine Learning Privacy Defenses are Misleading

Michael Aerni*
ETH Zurich
Switzerland

Jie Zhang*
ETH Zurich
Switzerland

Florian Tramèr
ETH Zurich
Switzerland

ABSTRACT

Empirical defenses for machine learning privacy forgo the provable guarantees of differential privacy in the hope of achieving higher utility while resisting realistic adversaries. We identify severe pitfalls in existing empirical privacy evaluations (based on membership inference attacks) that result in misleading conclusions. In particular, we show that prior evaluations fail to characterize the privacy leakage of the *most vulnerable samples*, use *weak attacks*, and avoid comparisons with *practical differential privacy baselines*. In 5 case studies of empirical privacy defenses, we find that prior evaluations underestimate privacy leakage by an order of magnitude. Under our stronger evaluation, none of the empirical defenses we study are competitive with a properly tuned, high-utility DP-SGD baseline (with vacuous provable guarantees).

1 INTRODUCTION

Machine learning models can memorize sensitive information from their training data, enabling privacy attacks such as membership inference [48] and data extraction [8]. Training with differential privacy [17]—in particular with DP-SGD [1]—provides provable protection against such attacks. Yet, achieving strong guarantees with good utility remains a challenge [19]. This has led to growing interest in *empirical* privacy defenses, which might offer a better privacy-utility tradeoff against practical attacks, but no formal guarantees [9, 12, 28, 39, 46, 52, 61].

Most evaluations of such empirical defenses for private machine learning use *membership inference attacks* [48] as the canonical approach to obtain a bound on privacy leakage. Under the notion of membership privacy, many heuristic defenses claim to achieve a better privacy-utility tradeoff than DP-SGD against state-of-the-art attacks [9, 12, 28, 52]. However, we find that such empirical evaluations can be severely misleading:

- (1) Current membership inference evaluations fail to reflect a model’s privacy *on the most vulnerable data*, and instead aggregate the attack success over a population. **But privacy is not an average-case metric!** [51] We show that *a blatantly non-private defense that fully leaks one training sample passes existing evaluations* (even with recent proposals to report an attack’s true-positive rate at low false-positive rates [4]).
- (2) Many defenses apply either a weak inference attack that does not reflect the current state-of-the-art [4, 63], or fail to properly *adapt* the attack to account for unusual defense components or learning paradigms. This issue is reminiscent of well-known pitfalls for non-adaptive evaluations of machine learning robustness [2, 54].
- (3) Empirical defenses are typically compared to *weak DP-SGD baselines* [9, 12, 28, 52] with utility below the state-of-the-art.

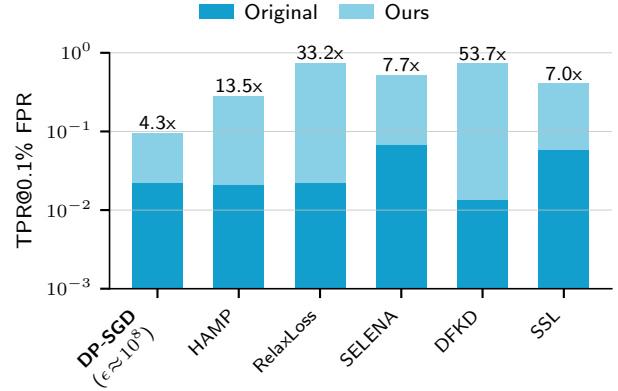


Figure 1: Empirical privacy evaluations provide a false sense of security. We study five heuristic defenses and a properly tuned DP-SGD baseline that all achieve $\geq 88\%$ accuracy on CIFAR-10. We first run a standard membership inference evaluation and report the attack’s TPR at a low FPR across the dataset (following [4]). Our new evaluation methodology, which adapts the attack to each defense and targets the least-private samples, reveals an order-of-magnitude higher privacy leakage. Our DP-SGD baseline provides better privacy (at similar utility) than all the empirical defenses.

To address the first issue, we introduce an efficient evaluation methodology that accurately reflects a defense’s privacy on the most vulnerable data points. Inspired by work on worst-case privacy auditing [7, 27], we inject canary samples that mimic the most vulnerable data, and focus our audit on those canaries only.

Then, for five representative empirical defenses, we design adaptive membership inference attacks based on LiRA [4], the state-of-the-art, and evaluate privacy using our new methodology. As Figure 1 shows, we reveal much stronger privacy leakage and a completely different ranking than the original evaluations suggest. None of the five defenses provide effective protection against properly adapted attacks targeted at the most vulnerable samples.

Finally, we show that none of these defenses are competitive with a strong DP-SGD baseline. By using state-of-the-art improvements to the original DP-SGD algorithm (e.g., [14]), and by tuning hyperparameters to achieve both high utility and high *empirical* privacy (at the expense of meaningful provable guarantees), we obtain a *better empirical privacy-utility tradeoff* than all other defenses.

Our work adds to the growing literature on pitfalls in evaluations of ML privacy defenses [5, 13, 57]. We aim to provide researchers a more principled evaluation framework, and an overview of pitfalls and misconceptions in existing evaluations. To promote reproducible research, we release all code for our evaluation methodology and our implementation of each empirical defense we study.¹

*Both authors contributed equally to this research.

¹<https://github.com/ethz-spylab/misleading-privacy-evals>

2 PRELIMINARIES AND RELATED WORK

2.1 Privacy Attacks

Machine learning models can memorize parts of their training data, enabling various privacy attacks. *Membership inference*—which we focus on in this work—corresponds to the most general form of data leakage: inferring whether a particular data point was part of a model’s training set [48]. Stronger attacks such as *attribute inference* [21] or *data extraction* [7, 8] aim to recover partial or full training samples by interacting with a model.

Membership inference attacks. In a membership inference attack, an adversary tries to guess whether some target sample was in the training data of a machine learning model.

Most membership inference attacks follow a common blueprint: For a trained model f and target sample x , the attack computes a score $\mathcal{S}(f; x)$, typically related to the training loss function (e.g., the sample’s negative cross-entropy loss). Then, the attack guesses that x is a member if $\mathcal{S}(f; x) > t$ for some threshold t .

Early membership inference attacks use a *global threshold* τ for all samples [48, 64]. A number of follow-up works highlight that a global threshold is suboptimal, as some samples are harder to learn than others [4, 45, 59, 63]. Thus, calibrating the attack threshold to each sample greatly improves membership inference.

The Likelihood Ratio Attack (LiRA). In this work, we build upon the LiRA framework of Carlini et al. [4], which frames membership inference as a hypothesis testing problem. Given a target sample x , LiRA models the score distributions under the hypotheses that x is a member of the training data, and that x is a non-member. Given the score of the victim model f on x , the attack then applies a *likelihood ratio test* to distinguish between the two hypotheses.

To estimate the score distributions, LiRA trains multiple *shadow models* [48] by repeatedly sampling a training set D (from the same or similar distribution as the training set of f), and training models f_{out} on D and f_{in} on $D \cup \{x\}$. Given sufficiently many shadow models, LiRA fits two Gaussians $\mathcal{N}(\mu_{x,\text{in}}, \sigma_{x,\text{in}}^2)$ and $\mathcal{N}(\mu_{x,\text{out}}, \sigma_{x,\text{out}}^2)$ to the scores from the “in” and “out” models on the target sample x . Finally, LiRA applies a standard Neyman–Pearson test to determine whether the observed score $\mathcal{S}(f; x)$ from the victim model f is more likely if x is a member or a non-member:

$$\mathcal{A}(f, x) := \frac{\mathcal{N}(\text{score}_x \mid \mu_{x,\text{in}}, \sigma_{x,\text{in}}^2)}{\mathcal{N}(\text{score}_x \mid \mu_{x,\text{out}}, \sigma_{x,\text{out}}^2)}, \text{ where } \text{score}_x = \mathcal{S}(f; x).$$

As an optimization, if the training algorithm relies on data augmentation, we can query the model on multiple augmentations of the target input x . LiRA then fits a multivariate Gaussian distribution to the corresponding scores. Follow-up work also considers querying models on additional samples (e.g., [60]), and improving the attack’s computational efficiency (e.g., [68]).

2.2 Privacy Defenses

Defenses against privacy attacks, in particular against membership inference, fall into two broad categories.

Provable defenses. A differential privacy (DP) [17] machine learning algorithm provably bounds the success of typical privacy attacks. Differentially private models are often trained using the DP-SGD algorithm [1], which protects each individual training step by

clipping and noising per-sample gradients. For many tasks, achieving strong provable privacy (e.g., $\epsilon \approx 1$) with DP-SGD requires a large noise magnitude, which deteriorates model utility.

If some *public* data is available, better privacy-utility tradeoffs are possible with techniques such as PATE [43], or public pretraining followed by private fine-tuning [14, 44, 53]. This paper focuses on the strict privacy setting, where all training data has to be protected.

Empirical defenses. Due to the high utility cost of provable privacy guarantees, many heuristic defenses aim for *empirical* privacy against realistic attacks. Existing heuristic defenses rely on techniques such as adversarial training [39], modifications to a model’s loss or confidence [9, 12, 28, 61], or indirect access to private features or labels (e.g., through distillation [52], self-supervised learning [11, 23], or synthetic data generation [16, 18, 35, 65]).

2.3 Empirical Privacy Evaluation

Membership inference evaluations. Membership inference (MI) attacks and defenses are typically evaluated on a dataset containing the victim model’s training data and an equal number of non-member samples. Early works on MI use average-case success metrics, such as the attack’s accuracy at guessing the membership of every sample in the evaluation set (see, e.g., [33, 48]).

Carlini et al. [4] critique this evaluation methodology, noting that it does not reflect an attacker’s ability to *confidently* breach the privacy of any individual sample. They instead propose to measure the attacker’s ability to infer membership—the true positive rate (TPR)—at a *low false positive rate* (FPR). Many recent works have adopted this metric (e.g., [3, 12, 60, 63, 68]). Yet, as we argue in this paper, reporting the TPR and FPR aggregated over a data population still fails to capture *individual privacy*, in particular for the *most vulnerable sample(s)*. We will thus instead propose a membership inference evaluation tailored to individual least-private samples. Similar metrics to ours appear in prior work (e.g., [6, 26, 34]), but not to empirically evaluate the privacy of defenses.

DP auditing. Differential privacy bounds an attacker’s ability to perform membership inference [29]. Specifically, for any dataset D and target sample x , a DP guarantee bounds the TPR-to-FPR ratio of any MI attack that distinguishes between a model trained on D vs. $D \cup \{x\}$. Crucially, the TPR and FPR here are calculated with respect to the randomness of the privacy mechanism (and attacker), but *not* with respect to a random choice of the dataset D or target sample x . Instead, DP provides a worst-case bound on membership inference for *every choice* of dataset and target sample.

This connection can be leveraged in the opposite direction—by using membership inference attacks to *lower-bound* the DP guarantees of an algorithm [27, 41, 50, 57]. These auditing mechanisms crucially differ from typical membership inference evaluations: to get the tightest bounds, DP auditing measures the attacker’s TPR and FPR solely for the least-private sample(s) (often referred to as “canaries” [7]), rather than over the entire data population.

3 PITFALLS IN PRIVACY EVALUATIONS

We identify three common pitfalls in existing empirical evaluations of privacy defenses. As mentioned in Section 2.3, existing evaluations typically rely on membership inference attacks, and report some aggregate measure of attack success across a standard dataset

(e.g., CIFAR-10). Additionally, many of these evaluations suggest that their empirical defense achieves significantly higher utility than a differentially private baseline (e.g., DP-SGD). We briefly review how existing evaluations lead to misleading empirical findings below, and propose an evaluation protocol that more accurately reflects a defense’s privacy in Section 4.

Pitfall I: Aggregating attack success over a dataset. Existing evaluations of membership inference attacks and defenses report privacy metrics that are aggregated over all samples in a dataset, either explicitly or implicitly.

Early evaluations (e.g., [40, 48, 64]) explicitly report average metrics such as attack accuracy or AU-ROC over a dataset of members and non-members. These metrics thus express the average leakage of a defense across the population. Carlini et al. [4] highlight a critical issue of such metrics: they fail to characterize whether an attacker can *confidently* infer membership of any sample (rather than, say, just guess better than random on average). Carlini et al. [4] thus propose to evaluate an attack’s true positive rate at a low false positive rate (e.g., 0.1%), that is, the fraction of members that the attack can identify while making only few errors on non-members.

Yet, we note that their evaluation methodology still computes an attack’s success at identifying membership (i.e., the TPR) *across all members*. That is, an attacker issues guesses *for all samples in the population*, and privacy leakage corresponds to the *proportion* of all training set members that are correctly identified (while controlling the rate of false positives over the entire data population). Informally, this evaluation thus captures *how many* records in a training set can be identified while keeping the number of false guesses over the population low.

We argue that this metric (and prior ones) fail to properly capture *individual privacy*. Indeed, existing metrics view privacy leakage as a property of a *data population*, rather than of each individual sample (i.e., does the model leak *my data*?). If a model violates the privacy of an individual, that individual likely does not care whether the model also leaks 0.1% or 10% of the remaining samples; the individual cares about the fact that an attacker can confidently recover *their* data. To make this point more concrete, we note that existing metrics can be arbitrarily “diluted” by adding new members for which a defense preserves privacy, even if the same defense fully leaks the membership of a fixed number of samples. We illustrate this point further in Section 4, where we showcase *a defense that fully violates one user’s privacy, yet passes existing evaluations*.

Pitfall II: Weak or non-adaptive attacks. Empirical defense evaluations aim to capture the privacy leakage under a realistic adversary. It is thus important that evaluations consider strong attacks which exploit all the capabilities of a presumed attacker. In particular, attacks must be *adaptive*, that is, fully know the defense mechanism, and adjust their attack strategy accordingly.

Yet, in practice, many empirical defense evaluations either use weak attacks that are no longer state-of-the-art, or fail to adapt the attacks to peculiarities of the defense. This situation is reminiscent of challenges in the field of adversarial examples, where early defense evaluations misleadingly suggest robustness using non-adaptive attacks (e.g., [2, 54]). For ML privacy, Choquette-Choo et al. [13] already show that some defenses explicitly or implicitly perturb a model’s loss to make standard membership inference

attacks fail, while remaining susceptible to different strategies. Yet, we find that the issue of weak and non-adaptive attacks still prevails among a number of empirical privacy evaluations.

Pitfall III: Comparison to weak DP baselines. Given that privacy defenses with theoretical guarantees exist (e.g., DP-SGD), a heuristic defense should demonstrate some clear advantage over them. Most existing works hence argue that their proposed defense provides a better empirical privacy-utility tradeoff² than DP-SGD—usually in the form of higher utility at reasonable privacy.

However, we find that privacy evaluations typically consider DP-SGD baselines that are incomparable to the proposed defense, since the DP baselines attain only a very low accuracy. For example, among the five evaluations in our case studies, none considers a DP-SGD baseline with more than 80% CIFAR-10 test accuracy.

The pitfall here is twofold: First, most defense evaluations only compare to “vanilla” DP-SGD (as proposed in [1]), without incorporating state-of-the-art techniques that can significantly boost utility (e.g., [14, 47]). Second, existing evaluations typically only compare to DP-SGD baselines that achieve “moderate” provable guarantees (e.g., $\epsilon \leq 8$). On datasets like CIFAR-10, such guarantees are not achievable alongside high utility with current techniques. Yet, since empirical defenses forgo provable guarantees anyhow, it makes sense to compare against a *heuristic* DP-SGD baseline with noise low-enough to achieve high utility. While such a heuristic DP-SGD instantiation will not provide meaningful privacy guarantees, it is a perfectly reasonable *empirical* defense to consider. Indeed, such heuristic DP uses are common in practice, with some deployments achieving only very weak guarantees (say $\epsilon = 50$) [15].

4 RELIABLE PRIVACY EVALUATION

To avoid misleading conclusions, we propose a reliable and efficient evaluation protocol for empirical ML privacy. Our protocol relies on three key points, each targeting one of the aforementioned pitfalls we identify in existing evaluations.

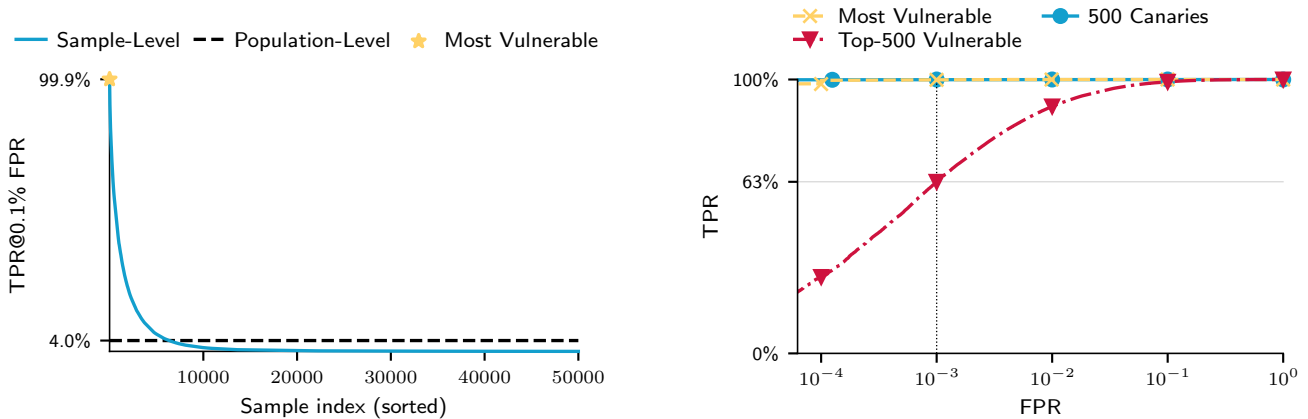
- (1) Evaluate membership inference success (specifically TPR at low FPR) for *the most vulnerable sample in a dataset*, instead of an aggregate over all samples. To make this process computationally efficient, audit a set of *canaries* whose privacy leakage approximates that of the most vulnerable sample.
- (2) Use a state-of-the-art membership inference attack that is properly adapted to specifics of the defense.
- (3) Compare to DP baselines (e.g., DP-SGD) that use state-of-the-art techniques and reach similar utility to the defense.

In the remainder of this section, we elaborate on each point, and discuss the practical implementation of our protocol.

4.1 Focus on the Most Vulnerable Samples

Most membership inference evaluations split a benchmark dataset D (e.g., CIFAR-10) into two disjoint sets of members D_{in} and non-members D_{out} (typically of equal size), and apply a membership inference attack \mathcal{A} . Given a model f trained on D_{in} and a target sample $x \in D$ as input, the attack outputs a membership score $s \leftarrow \mathcal{A}(f, x)$ that indicates the attacker’s confidence of x being

²A defense could also aim to be more computationally efficient than DP-SGD, but few empirical defenses claim this as a main goal. Moreover, we find that the computational cost of heuristic DP-SGD baselines is close to the most efficient defenses we study.



(a) Population-level evaluations fail to capture the privacy leakage of the most vulnerable samples. We compare the TPR@0.1% FPR of LiRA on every CIFAR-10 sample in isolation (sample-level) to an aggregate over all samples (population-level, as in Carlini et al. [4]). The attack’s success at inferring membership of the most vulnerable sample is orders of magnitude higher than the attack’s success at inferring membership across the dataset.

(b) Well-chosen canaries are crucial to capture privacy of the most vulnerable sample. Measuring success over the top-500 most vulnerable samples (red) severely underestimates the worst-case privacy leakage (yellow) because the sample-level TPRs in (a) decay rapidly. However, our well-chosen canaries (blue, mislabeled samples in this instance) closely approximate the most vulnerable sample in terms of attack success.

Figure 2: Membership inference evaluations should focus on the leakage of the most vulnerable sample(s), which can be approximated efficiently using a canary set. In (a), we train 20,000 shadow models on CIFAR-10 to compute the MI attack success (TPR at 0.1% FPR) *independently for each individual sample*. We find that the most vulnerable sample is considerably easier to attack than a population-level evaluation suggests. In (b), we show that constructing an appropriate canary set allows us to capture the worst-case privacy leakage in a computationally efficient manner. Note that both plots use a linear y-axis; see Appendix A.2 for experimental details.

a member of the training set. Crucially, existing evaluations then quantify privacy leakage via the aggregated attack success *on every sample in D* —for example, by computing an ROC curve over the attacker’s confidence on all samples. Such evaluations thus measure the *fraction of samples* an attacker can confidently identify.

We argue that this measure fails to capture the privacy of each individual sample. In particular, for existing evaluations, a model’s purported privacy can be arbitrarily *improved* by adding “safe” examples to the dataset, even though the leakage of the most vulnerable samples does not change. We illustrate this phenomenon with an extreme example below.

Name and shame: A blatantly non-private defense that passes existing privacy evaluations. Consider the following simple “name-and-shame”³ defense $NS_{\hat{x}}$ that fully leaks the membership of one fixed target sample \hat{x} :

$$NS_{\hat{x}}(D_{\text{in}}) = \begin{cases} 1 & \text{if } \hat{x} \in D_{\text{in}}, \\ 0 & \text{otherwise.} \end{cases}$$

That is, the defense $NS_{\hat{x}}$ outputs 1 if and only if the target \hat{x} is in the training set (obviously, this does not yield a useful ML model). This defense completely violates the membership privacy of \hat{x} , while fully protecting all other training samples.

If we evaluate any MI attack over the entire dataset D of members and non-members, we get that

$$\text{TPR} \leq \text{FPR} + 1/|D|.$$

³Such mechanisms often appear in discussions of (ϵ, δ) -differential privacy [49] to motivate the need for the parameter δ to be much smaller than the size of the dataset.

Thus, in existing evaluations, this defense can be made arbitrarily private by increasing the size of D . Evaluating on more samples indeed improves the defense’s privacy *on average* across the population (i.e., a smaller proportion of the dataset is at risk of privacy leakage); yet, from the individual perspective of \hat{x} , the defense never provides any privacy at all.

Privacy is non-uniform in practice. The name-and-shame defense is pathological, but illustrates an important point: the *proportion* of samples whose privacy is violated does not reflect the privacy leakage of the *most vulnerable samples*. We now show that this issue also affects privacy measurements on typical ML datasets.

We consider the standard setting from Carlini et al. [4] where the victim model f is trained on a dataset D_{in} containing half of the samples from the CIFAR-10 training set (i.e., 25,000 training points). We run the LiRA attack \mathcal{A} with 64 shadow models trained on random splits of CIFAR-10, and evaluate the results in two ways: (1) *Population-level*: We apply the attack to each of the 50,000 samples in the CIFAR-10 dataset $D = D_{\text{in}} \cup D_{\text{out}}$, and report the TPR at 0.1% FPR across all samples—the original setting of Carlini et al. [4]. More precisely, we define

$$\text{TPR}(T) := \Pr_{x \sim D_{\text{in}}} [\mathcal{A}(f, x) > T], \quad \text{FPR}(T) := \Pr_{x \sim D_{\text{out}}} [\mathcal{A}(f, x) > T],$$

and select the threshold T as

$$T = \arg \max_t \{ \text{FPR}(t) \leq 0.1\% \}.$$

In words, we set the threshold so that the attack makes false membership guesses for at most 0.1% of the non-members, and then report the *proportion* of all members that are correctly identified.

(2) *Sample-level*: We compute the attack’s TPR and FPR for each sample *individually*. To do this, we perform the MI experiment 20,000 times by repeatedly resampling half of the CIFAR-10 training set, and fitting a model on the resulting D_{in} .⁴ For each sample x in the full CIFAR-10 training data, we then define

$$\begin{aligned} \text{TPR}_x(T_x) &:= \Pr_{D_{\text{in}}, f \sim \text{Train}(D_{\text{in}})} [\mathcal{A}(f, x) > T_x \mid x \in D_{\text{in}}], \\ \text{FPR}_x(T_x) &:= \Pr_{D_{\text{in}}, f \sim \text{Train}(D_{\text{in}})} [\mathcal{A}(f, x) > T_x \mid x \notin D_{\text{in}}], \end{aligned}$$

and select sample-specific attack thresholds T_x as

$$T_x = \arg \max_t \{ \text{FPR}_x(t) \leq 0.1\% \}.$$

That is, we now set the (sample-specific) attack threshold so that the attack makes at most 0.1% of false membership guesses for that specific sample, *across multiple possible training runs*. Then, we report the probability of the attacker correctly inferring membership (again, taken over multiple training runs).

In Figure 2a, we rank all CIFAR-10 samples by their individual TPR at 0.1% FPR (sample-level), and compare those values to the TPR at 0.1% FPR when aggregating attack success across all the full dataset (population-level). The results confirm that, even in CIFAR-10, a small fraction of samples is significantly more vulnerable to membership inference than the average data point. In particular, the TPR at 0.1% FPR of the most vulnerable sample is 99.9%—orders of magnitude higher than the population-level metric (4%) suggests.

Our proposed evaluation metric: TPR at low FPR for the most vulnerable sample. We thus argue that empirical evaluations of privacy defenses should target membership inference attacks at the most vulnerable sample in a dataset,⁵ and report the corresponding TPR at a low FPR. Our metric answers how likely a real-world attacker is to confidently identify *a specific sample* in the dataset, instead of measuring leakage across the entire population.

This metric reconciles empirical MI evaluations with the privacy semantics of DP, which guard against reliable membership inference for *any* individual sample, regardless of how private a defense may be on other samples. Our approach also accurately captures privacy of the “name and shame” defense: for the most vulnerable sample, our metric yields a TPR of 100% at 0% FPR; thus, the “name and shame” defense clearly fails to pass our evaluation.

Efficient approximation using canaries. Ideally, our privacy evaluation would directly estimate the TPR at a low FPR for the most vulnerable sample(s) in a dataset by repeating the membership inference attack many times. However, this is computationally highly expensive: to estimate an attack’s TPR at FPR α , even for a single sample, we need to run the attack $O(1/\alpha)$ times.

If we train S models and evaluate the attack on C samples, we thus want $S \cdot C \gg 1/\alpha$, introducing a tradeoff between tightness of the privacy bound and computational efficiency. Existing works mainly focus on two extremes:

- Standard MI evaluations run the attack on the full dataset D (i.e., $C = |D|$). Hence, even a small number of victim models S (as few as one) can provide sufficient statistical power if the dataset is large. Yet, as previously discussed, this approach yields a population-level measure of privacy.
- Techniques for DP auditing [41, 57] often evaluate the attack on a single worst-case sample (i.e., $C = 1$), and must thus train $S \gg 1/\alpha$ models for a strong privacy bound. At a typical FPR of $\alpha = 0.1\%$, this corresponds to training thousands of models.

Our (illustrative) approach in Figure 2a follows the latter extreme: we used 20,000 models to tightly approximate the per-sample attack success at low FPRs. Such an approach is of course impractical in general, especially since many privacy defenses add computational overhead over standard training.

We thus adopt a natural middle ground: we evaluate membership inference on a small set of $1 \ll C \ll |D|$ samples (called “canaries” [7]), where each canary is inserted independently at random in the training data of a small number S of models. The evaluation then reports membership inference success only over the canary set, ignoring the remaining data.

Crucially, we design canaries to mimic the most vulnerable samples in the data, instead of simply selecting a subset of the data (either at random, or in decreasing order of vulnerability). This ensures that an attack’s performance on canaries approximates (or upper-bounds) the performance on the most vulnerable sample. Figure 2b highlights the importance of properly designed canaries. Here, we choose a set of $C = 500$ canaries and train $S = 64$ models, which allows us to reliably measure FPRs on the order of 0.1% over the canary set. If we were to simply pick 500 samples from the dataset at random, we would obtain a TPR at 0.1% FPR close to that computed over the full dataset (i.e., $\approx 4\%$). One might hence be tempted to use the 500 most vulnerable samples. However, due to the small number of highly vulnerable samples, this approach still underestimates the TPR@0.1% FPR of the least-private sample (63% vs. 99.9%). If we instead design an appropriate canary set (random mislabeled samples from CIFAR-10 in this case), we can closely approximate the ROC curve of the most vulnerable sample—but crucially, only train 64 models instead of 20,000 (as in Figure 2a).

Our approach is similar to the DP auditing procedure proposed by Steinke et al. [50]. While they focus on “extreme” computational efficiency by auditing an algorithm using just one single training run (i.e., $S = 1$), we repeat the training algorithm multiple times to obtain tighter empirical privacy estimates using the LiRA attack. As we discuss in the following, the tightness of the estimate ultimately hinges on an appropriate choice of the membership inference attack and canary set—both depending on the specifics of the defense.

4.2 Adapt Attacks and Canaries to the Defense

Reliable defense evaluations must adapt their attacks and canary choice to the defense. Indeed, a robust defense should protect the most vulnerable samples against the strongest adversary within its threat model. Yet, the nature of the most vulnerable samples, and of the strongest attack, may depend on specifics of the defense.

Adapting attacks. State-of-the-art membership inference attacks rely on the assumption that a model’s loss (or confidence)

⁴We thank Matthew Jagielski for providing us with these models.

⁵We could also consider a fully adversarial dataset and target sample, as often done for auditing DP implementations [41, 57]. Yet, the rationale for heuristic defenses is precisely that such worst-case scenarios are unrealistic in practice. In keeping with this motivation, we thus aim to measure the privacy that a defense confers for “natural” datasets and samples, but while focusing on the most vulnerable of these samples.



Figure 3: Mislabeled, ambiguous, and atypical samples are most vulnerable to privacy attacks. The most vulnerable CIFAR-10 samples in the setting of Figure 2a are images that are mislabeled (e.g., humans labeled “truck”), ambiguous (e.g., a bird on a car), or atypical (e.g., a boat on land or an airplane without wings). See Appendix B.5 for more samples and $\text{TPR}@0.1\% \text{ FPR}$ values.

on a sample contains the strongest membership signal. However, some defense designs might violate this assumption.

One well-known example is *confidence masking* [13], where a defense explicitly obfuscates model predictions at deployment-time. Choquette-Choo et al. [13] show that such defenses are vulnerable to adaptive label-only attacks, that is, attacks that only rely on a model’s predicted label (which those defenses preserve).

More broadly, generic membership inference attacks may be inadequate for defenses that depart the standard supervised training regime. For example, consider a defense based on self-supervised learning that first trains an encoder using unlabeled data, followed by a simple supervised fine-tuning stage. For such a defense, memorization could occur in either of the two training stages, but a generic attack such as LiRA might fail to fully exploit memorization of unlabeled data during pretraining. Similar concerns might arise for other multi-stage defenses, for example, ones that use synthetic data generation or distillation.

Adapting canaries. Recall that the purpose of canaries in our evaluation protocol is to construct a set of samples such that (1) the privacy leakage for the population of canaries approximates the leakage of the most vulnerable sample in the dataset, and (2) the set is large enough to obtain a robust measure of low attack FPRs (e.g., 0.1%) with a reasonable number of models.

Which samples are particularly vulnerable typically depends on the type of defense that is employed. Similarly, a defense might affect the interactions between different canaries that are simultaneously present in the training data. As a result, a good choice of canary is inherently defense-dependent. Figure 3 highlights some of the most vulnerable CIFAR-10 samples for standard training, that is, the samples with the highest $\text{TPR}@0.1\% \text{ FPR}$ in Figure 2a. These examples suggest that atypical images (e.g., a ship on land) and mislabeled samples (e.g., humans labeled as “truck”) are strong canary candidates for CIFAR-10—at least for undefended models.

However, we must also consider interactions between canaries. For example, suppose we use many pictures of “boats on land” as canaries. Those will no longer be “atypical”, as the model will learn to

generalize to such images. As a result, each individual canary might exhibit significantly less memorization than the most vulnerable sample in the original CIFAR-10 dataset. We thus want canaries whose privacy leakages are as independent as possible from one another. That is, the inclusion of one canary in the dataset should minimally influence the model’s ability to fit the other canaries.

Mislabeled samples are a strong default candidates for canaries; indeed, such samples are common in DP auditing [41, 50]. If we choose the incorrect labels at random, a model provably cannot generalize to the canary set. As long as the canary set is reasonably small, using mislabeled samples also minimally affects a model’s utility. Hence, for standard supervised learning, mislabeled samples satisfy both desiderata for good canaries, and approximate the most vulnerable sample in the original dataset well.

Yet, similar to attacks, the choice of canaries crucially depends on both the dataset *and the defense*. For example, as we discuss in Section 5.4, defenses that ignore label information are not vulnerable to mislabeled samples. Hence, a robust empirical defense evaluation must adapt its canaries to the defense. Doing so requires a careful analysis of the defense mechanism, either analytically or through a form of red teaming; systematically determining strong canaries for any given defense is still an open problem. We hence illustrate a heuristic approach using our case studies.

4.3 Use Strong DP Baselines

Since defenses with provable DP guarantees exist, heuristic defenses should provide some distinct practical advantage over them. In this paper, we focus on the presumed utility advantage: heuristic defenses claim to provide higher accuracy than DP algorithms, while still defending against realistic adversaries.

Forgoing theoretical guarantees for practical advantages is common in computer security. For example, empirical defenses against adversarial examples (such as adversarial training [36]) are often preferred over techniques with provable robustness, as the former yield higher accuracy models while still defending against all known attacks. More broadly, many practical deployments of cryptographic algorithms rely on techniques with no theoretical guarantees (e.g., hash functions like SHA-3, or symmetric encryption like AES)—even though there exist (much more expensive) schemes whose security can be provably reduced to a well-characterized mathematical problem (e.g., factorization).

While the first two principles of our methodology focus on properly evaluating heuristic defenses, our third principle calls for a more rigorous comparison with provable baselines. In particular, empirical privacy evaluations should compare heuristic defenses to state-of-the-art DP baselines at a comparable utility level.

Focus on high utility regime. Existing defense evaluations typically use a DP-SGD baseline with low utility and moderately strong provable privacy guarantees (e.g., ϵ often around 4–8).

Yet, a defense with a drastic utility cost is unlikely to be used in practice. We hence argue that a comparison to low-utility DP baselines is unwarranted. Moreover, since heuristic defenses forgo theoretical guarantees anyhow (under the assumption that these guarantees are loose in practice), there is no reason to hold DP baselines to the higher standard of proper provable guarantees.

We thus instead propose to tune DP baselines such that they (1) attain some minimal utility, comparable to that of the heuristic defense, and (2) maximize empirical privacy under this utility constraint. Notably, we do *not enforce meaningful provable guarantees*, and potentially treat DP-SGD as a purely empirical defense.

Use state-of-the-art DP-SGD methods. The “vanilla” DP-SGD algorithm of Abadi et al. [1] employs a similar training setting as standard supervised learning models, with the addition of gradient clipping and noising. Many works show that certain techniques can substantially improve the utility of DP-SGD while retaining the same privacy guarantees [14, 47] (e.g., by using a different data augmentation strategy). A fair evaluation should thus account for these state-of-the-art methods when comparing to DP-SGD.

Overall, we note that the current literature rarely studies DP-SGD in the high-utility regime (e.g., > 91% accuracy on CIFAR-10). One potential reason is that achieving very high utility currently requires hyperparameters (e.g., batch size and noise magnitude) that yield meaningless worst-case guarantees (e.g., $\epsilon > 10^8$). Yet, even without provable privacy, DP-SGD constitutes a perfectly valid heuristic defense—which we find to consistently outperform other methods in our case studies.

5 CASE STUDY EXPERIMENTS

We now illustrate pitfalls in defense evaluations and motivate our evaluation strategy among five diverse empirical defenses against membership inference. We first briefly introduce these defenses and our experimental setup in Sections 5.1 and 5.2, respectively. We then instantiate the three prongs of our evaluation strategy: (1) we develop strong adaptive attacks in Section 5.3; (2) design strong canaries for each defense in Section 5.4; and (3) compare these empirical defenses with DP-SGD in Section 5.5 (and show that none are competitive with a properly tuned DP-SGD baseline).

We do not claim that the attacks or canaries we design for each defense are optimal, but they suffice to highlight the stark differences between our proposed focus on the most vulnerable sample compared to weaker, non-adaptive population-level evaluations.

5.1 Defenses

The five defenses we study fall into two categories: four are peer-reviewed defenses that explicitly aim to protect privacy, and one is a “folklore” defense that illustrates how departing from a standard supervised learning setting can impede state-of-the-art attacks. We omit certain well-known empirical membership inference defenses [16, 28, 39, 61] that have been circumvented in prior work [5, 13].

HAMP. HAMP [12] combines training-time modifications (i.e., entropy regularization and label smoothing; not important for our attacks) and a test-time defense that explicitly randomizes a model’s confidence. Specifically, given a trained model f and input image x , the defense output a *random* confidence vector such that the order of predicted classes matches the original prediction $f(x)$. This is an obvious case of *confidence masking* [13].

RelaxLoss. RelaxLoss [9] reduces overfitting by constraining the training loss to be above a fixed threshold. Concretely, for every training batch, the defense first computes the cross-entropy loss $\ell_{\text{batch}} = 1/B \sum_{i=1}^B \mathcal{L}(x_i, y_i)$ as in standard training. Then, RelaxLoss

compares the batch loss to a target loss threshold ℓ_τ : If $\ell_{\text{batch}} > \ell_\tau$, the defense continues with standard gradient descent; however, if $\ell_{\text{batch}} \leq \ell_\tau$ then RelaxLoss instead takes a (modified) gradient ascent step, with the goal of raising the loss above ℓ_τ .

Self Ensemble Architecture (SELENA). SELENA [52] is a distillation defense that heuristically mimics the provable guarantees of PATE [43], without the need for public data or noise addition. SELENA first splits the training data into (partially overlapping) chunks D_1, D_2, \dots, D_k and independently trains one teacher model f_i on each chunk. In a second distillation stage, the defense trains a model f_{student} using the soft predictions from the k teacher models. To promote membership privacy, for every sample x , SELENA only distills soft prediction from the teachers f_i that were *not* trained on x (i.e., $x \notin D_i$). The rationale is that f_{student} is trained to mimic the responses of the teachers on non-members only.

Data-Free Knowledge Distillation (DFKD). DFKD [10, 35, 65, 70] transfers knowledge from a teacher model—trained on private data—to a student model trained solely using *synthetic data*. While data privacy is a primary motivation for DFKD, we are not aware of prior work evaluating this defense against membership inference attacks (some works argue privacy by visually comparing the synthetic data to the training data [22, 69]). As a representative from this line of work, we study the state-of-the-art method of Fang et al. [18]. At a high level, their method proceeds in four steps: (1) train a teacher model f on the private training set; (2) train a generative model to produce synthetic data using an inversion loss (e.g., by matching the batch-normalization statistics of the teacher model); (3) distill a student model f_{student} using synthetic images from the generator and soft labels from the teacher model; (4) repeat steps 2 and 3 iteratively until the model converges. The privacy intuition is that the student model only observes noisy synthetic data, not the original (private) training data. Yet, as we will see, such “visual” privacy arguments can be highly misleading.

Self-Supervised Learning (SSL). Self-Supervised Learning is a technique to learn feature representations from unlabeled data. Given a labeled dataset $\{(x_1, y_1), \dots, (x_n, y_n)\}$, the SSL defense first trains a feature encoder ϕ in an unsupervised fashion, using only the features $\{x_1, \dots, x_n\}$. We consider two popular methods, SimCLR [11] and MoCo [23], both employing a contrastive loss which ensures that different *augmentations* of an input yield similar features (i.e., $\phi(x) \approx \phi(\text{aug}(x))$). Then, in a second stage, we train a linear classifier $f(x) = W\phi(x) + b$ on top of the frozen encoder, using the full labeled training set and a standard cross-entropy loss. SSL is not explicitly a defense against membership inference, but has received a lot of study regarding its privacy [25, 30, 32]. We include this SSL-based defense to illustrate a shortcoming of a naive privacy evaluation that applies a LiRA-like attack out-of-the-box without accounting for the unsupervised nature of the encoder’s training.

5.2 Experimental Setup

Dataset. We run all experiments on CIFAR-10 [31], a canonical benchmark dataset used by most existing empirical evaluations of privacy defenses. Due to the relatively high computational cost of our experiments, we refrain from studying more datasets and focus

our efforts on a single one. As our goal is to reveal pitfalls in existing evaluations, we believe that case studies on the most standard dataset used in the field are sufficient. Similarly, previous works on pitfalls in adversarial robustness evaluations typically use a single dataset to show that existing evaluations are incomplete [2, 54].

Shadow models and audit samples. Similar to Carlini et al. [4], we train multiple models on random subsets of the CIFAR-10 training set. However, rather than subsampling the entire training set as in [4], we follow Steinke et al. [50]: we designate 500 random data points as “audit samples” on which we evaluate membership inference; we always include the remaining 49,500 samples in every model’s training data.⁶ For population-level evaluations, we attack these audit samples as-is (since the audit samples are a random sample from the population, the expected attack success on the audit samples is the same as on the full population). For our evaluation that focuses on the most vulnerable samples, we replace the 500 audit samples with appropriately chosen canaries.

For each defense, we train 64 models, randomly including each audit sample in exactly half of the models’ training datasets. For evaluation, we use a leave-one-out cross-validation (as in [56]), where we evaluate the attack 64 times, once with each model as the victim and the remaining 63 models as the attacker’s shadow models. We then calculate the attack’s TPR and FPR over the $64 \cdot 500$ guesses of the attacker on all canaries and victim models.

To control for randomness in our evaluation, all experiments use the same non-audit samples, shadow model assignments, and audit samples given a fixed choice of canaries. Hence, two experiments using the same type of canaries use exactly the same data; datasets with different canaries are identical up to the 500 audit samples.

Defense implementation. We further control neural network architecture and capacity: all defenses except SSL use a WRN16-4 base model [67]; for SSL, we could not achieve sufficiently high utility with the WRN16-4 architecture, and thus follow [11, 23] by using a ResNet-18 [24] instead.

Moreover, we re-implement all defenses (carefully following all original design decisions). This allows us to use exactly the same setting in all case studies, and enables straightforward reproducibility of our results. We then tune all privacy-related defense hyperparameters (where available) to maximize privacy constrained to at least 88% CIFAR-10 test accuracy, and otherwise use the values proposed in each defense’s original paper. See Appendix A.4 for specific hyperparameters and implementation details.

LiRA attack. For LiRA, we always report the maximum TPR@0.1% FPR over the strongest approaches proposed in [4]. More precisely, we consider the Hinge vs. Logit scores, and attacking just the original sample vs. 18 augmented versions (since not all defenses employ data augmentation). The augmentations consist of horizontal flips, and shifting images by ± 4 pixels on each axis.

5.3 Adaptive Attacks

A reliable privacy evaluation must use the strongest possible attack in a given threat model. We hypothesize that for two defenses

in our case studies—SSL and HAMP—the standard LiRA attack is not strong, because both defenses violate some of the attack’s implicit assumptions. We thus develop custom attacks tailored to the specifics of SSL and HAMP. While we do not claim either attack to be optimal, our simple adaptations suffice to highlight how evaluations using weak attacks can yield misleading results.

Adapting attacks to contrastive losses in SSL. SimCLR and MoCo, the two SSL techniques that we consider, train an encoder neural network ϕ using a contrastive loss to learn representations from *unlabeled* images. The full defense trains an additional linear classifier on top of this (fixed) encoder, using the private labels.

We hypothesize that the cross-entropy loss of the full defense encodes only a weak membership signal, since this loss is only used to train the final layer. Thus, applying LiRA out-of-the-box to the full defense is unlikely to be effective. This has also been highlighted in concurrent work [58], which shows that SSL encoders tend to memorize training images despite not using any labels for training. We hence adapt LiRA to the SSL setting by specifically targeting the contrastive loss used to train the encoder.

When training an encoder, both MoCo and SimCLR maximize the similarity between representations of augmented version of the same image (positive pairs), and minimize the similarity between augmented versions of different images (negative pairs). We thus expect that representations of an image under different augmentations are more similar if that image is a training member—analogous to overconfident predictions in supervised learning.

Specifically, given a target image, we apply two random augmentations to the image, and calculate the cosine similarity between the corresponding defense outputs.⁷ We consider two attack variants here: (1) a white-box attack that directly computes similarity over the outputs of the *encoder* ϕ ; (2) a black-box attack that applies the contrastive loss to the logits output by the full defense (including the linear classifier). Finally, to account for randomness in the data augmentations, we repeat this procedure six times for every image, and average the similarities.

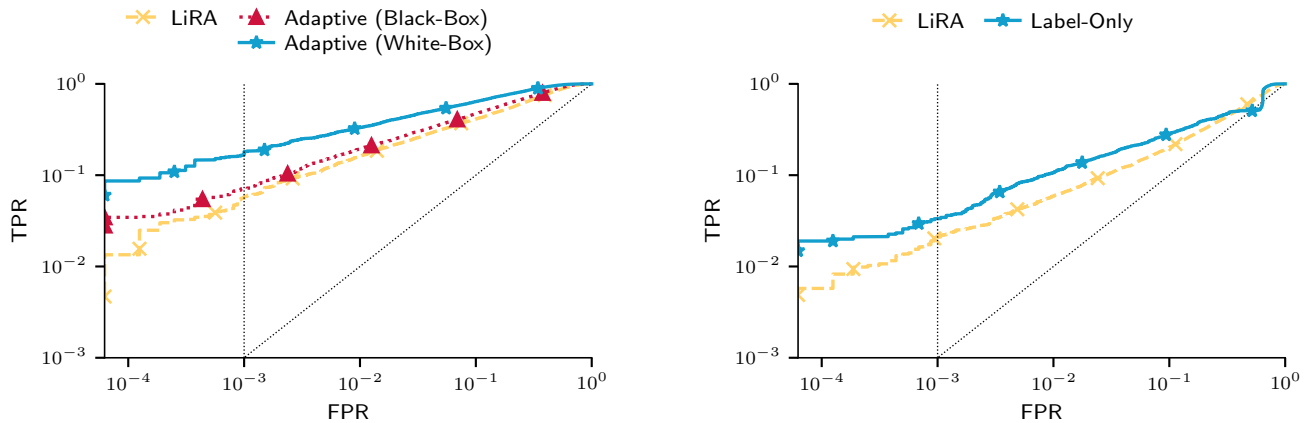
The results in Figure 4a (for SimCLR) support our hypothesis that most memorization happens during self-supervised training. Directly attacking the SSL encoder (white-box) using our adaptive attack yields a threefold increase in privacy leakage compared to standard LiRA on the full defense. In a black-box setting, our adaptation of the attack’s loss increases the TPR against the full defense from 5.8% to 7.1% (at a FPR of 0.1%). In the remainder of this section, we build upon the stronger white-box attack, and present black-box results in Appendix B.1.

While our results already highlight the importance of strong adaptive attacks, more sophisticated strategies might reveal even higher privacy leakage. Indeed, our current attack only considers the positive part of the contrastive loss (i.e., similarity between two augmentations of an image), while ignoring the negative part (i.e., dissimilarity between augmentations of different images).

An orthogonal, but interesting observation from this experiment is that there do exist defenses where a white-box MI adversary outperforms a black-box attacker. As noted by Carlini et al. [4], it

⁶Fixing most of the training data may put adversaries at an advantage, as the shadow models and target models are more similar in our setting. Yet, we show in Appendix A.3 that this has a negligible effect on attack success rates.

⁷Since the cosine similarity is a value $\rho \in [-1, 1]$, we apply a Fisher transformation, $\log(1 + \rho)/(1 - \rho)$, to obtain empirically normally distributed statistics.



(a) *Adapting to the pretraining loss yields a stronger attack for SSL.* In both a black-box (attacking the final classifier) and especially in the white-box setting (directly attacking the SSL encoder), our score that exploits contrastive losses increases the success of the standard LiRA attack. We only present the SimCLR-based defense for brevity; see Appendix B.1 for MoCo.

(b) *A label-only attack circumvents confidence masking in HAMP.* The test-time defense provides good privacy against state-of-the-art confidence-based attacks such as LiRA (yellow), but our simple label-only attack (blue) achieves almost threefold privacy leakage. See Appendix B.2 for more details.

Figure 4: Adaptive membership inference attacks that exploit defense-specific mechanisms improve over the standard LiRA attack. We show results for the (a) SSL and (b) HAMP defenses, with LiRA evaluated across the entire dataset.

remains unknown whether we can build stronger white-box attacks for standard supervised learning defenses.

Circumventing confidence masking in HAMP with label-only attacks. In contrast to SSL, HAMP uses a fairly standard supervised learning approach, for which LiRA is appropriate. However, since the defense actively obfuscates the model’s predicted confidences at test time, the standard attacks achieve a low TPR of only 2.1% at 0.1% FPR. This (presumed) protection stems primarily from HAMP’s test-time defense, as the same attack on non-obfuscated predictions is significantly stronger (see Appendix B.2).

The test-time defense erases all information in model predictions besides the predicted label order, thereby performing *confidence masking* [13]. We hence follow Choquette-Choo et al. [13], and develop a straightforward label-only attack.

Our attack queries the model on 18 fixed data augmentations of the target sample, and checks whether the model classifies each input correctly. This yields a binary vector of 18 entries. Using the shadow models, we then fit a logistic regression classifier, which takes this binary vector as input, and predicts membership of the target sample. Finally, we use the confidence of each classifier as a membership score $\mathcal{A}(f; x)$, and calculate the usual TPR and FPR statistics. See Appendix A.4 for further details.

Figure 4b compares our label-only attack with standard LiRA. Our adaptive label-only attack achieves a consistent increase in TPRs compared to the original LiRA attack. Based on the results in [13], we conjecture that computationally more expensive label-only attacks (e.g., using strategies from black-box adversarial example attacks) would be even stronger. But, as we will see in Section 5.4, our simple adaptive attack suffices to break the privacy of HAMP on the most vulnerable samples.

Other defenses. The other heuristic defenses we study (Relaxloss, SELENA and DFKD) use more standard supervised learning

methods, without any obvious confidence masking. We thus apply the original LiRA attack to these, and show in the following section that this suffices to breach privacy of the most vulnerable samples.

Nevertheless, it is possible that stronger adaptive MI attacks exist for some of these defenses. In particular, DFKD’s use of generative modeling and synthetic data introduces a layer of indirection that could be exploited. However, our attempts at building a stronger attack than LiRA for this defense were unsuccessful.

5.4 Sample-Level Privacy using Canaries

We now focus on the most important part of our evaluation protocol: measuring the attack success on the most vulnerable samples in a dataset, rather than on the dataset as a whole. Recall that evaluating attack success on each sample independently would be computationally expensive, as it requires thousands of shadow models. We instead measure the attack’s success on a set of canaries that are designed to mimic the (suspected) most vulnerable sample.

Figure 5 provides a summary for all our case studies. We consistently find that approximating the most vulnerable samples using defense-specific canaries yields a TPR@0.1% FPR that is between 2× and over 50× higher compared to population-level evaluations on a random CIFAR-10 subset. Crucially, our evaluation substantially changes the ranking between defenses: DFKD, for example, appears to be one of the most private defenses when success is aggregated over the full dataset, yet exhibits the second-worst privacy leakage for the most vulnerable samples. We discuss our canary choices (Table 2 in the appendix) and stress the importance of adapting canaries to evaluated defenses in the remainder of this section.

Mislabeled samples are a strong baseline. As discussed in Section 4.2, mislabeled samples are a good default choice of canaries. Intuitively, those samples are naturally vulnerable to membership inference in supervised learning: a model capable of memorization

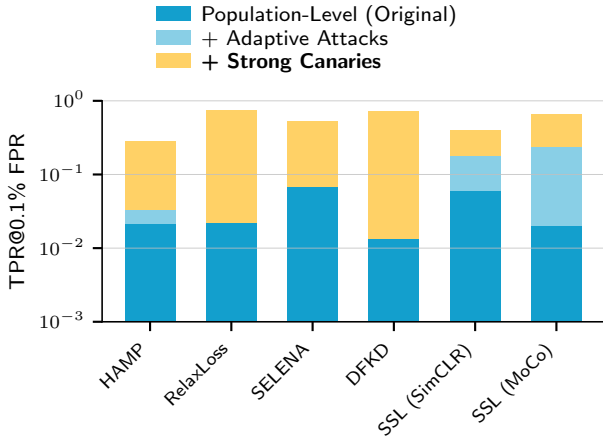


Figure 5: Our improved evaluation uncovers substantial privacy leakage for the most vulnerable samples. While most defenses appear private at the population-level (original), our evaluation with strong adaptive attacks targeted at defense-specific canaries reveals large privacy leakage for the most vulnerable samples. Note that the defense that appears to be the most private on a population-level (DFKD) is the second-least private on a sample-level!

and generalization will tend to assign high confidence to the wrong class if a mislabeled sample is a training member (memorization), but low confidence if the sample is not in the training data (generalization). Because practical datasets tend to contain some label noise (e.g., [37, 42, 71]), mislabeled samples may hence approximate the most vulnerable samples in such datasets well.

To generate mislabeled samples as canaries, we independently change the labels of all 500 audit samples to a uniformly random new class. For HAMP, RelaxLoss, and DFKD, a MI attack on those canaries yields a TPR@0.1% FPR of around 30% to 70% in Figure 5.

For DFKD in particular, this highlights the importance of rigorous privacy evaluations, compared to visual inspections or intuitions (as done in some prior work [22, 69]). Even though DFKD’s distillation process uses synthetic data—and hence omits wrong labels—the defense exhibits a TPR@0.1% FPR of 72.2%. We defer a more detailed investigation to future work, and now focus on two defenses that are robust against label noise: SSL and SELENA.

Out-of-distribution images are strong SSL canaries. Real-world data is often long-tailed, that is, it contains many “typical” samples, and few outliers (e.g., mislabeled or atypical images). For standard supervised learning, Feldman [19] argues that the only way to fit outliers and perform well on similar test samples is by memorizing labels. However, self-supervised learning itself solely relies on unlabeled data; changing a sample’s class does hence not influence memorization. We thus hypothesize that our SSL defenses, which heavily rely on pretraining with unlabeled data, do not memorize most label noise. In fact, we find that both SSL defenses have an average training accuracy on mislabeled canaries of only 1.3%—significantly below random guessing (10%).

Hence, we consider *atypical images* as a different type of outliers. Indeed, recent work by Wang et al. [58] found that SSL feature

encoders tend to memorize atypical images, and such memorization can be necessary for good downstream generalization.

However, since rare images constitute only a small fraction of CIFAR-10 by definition, we use a proxy as canaries: *out-of-distribution (OOD) data*. More concretely, we replace the original audit set with 500 downsampled ImageNet images. To decrease correlation between canaries, we pick each sample from a different ImageNet class, and assign labels independently at random.

The results in Figure 6a confirm our hypothesis, and highlight how the choice of canaries depends on the specifics of a defense. In a white-box setting, our attack on OOD canaries achieves a TPR@0.1% FPR as high as 65%—between 2.2× and 2.7× times higher than on the original/mislabeled audit set.

The choice of canaries is even more important in the black-box setting. Indeed, mislabeled samples yield a slightly *lower* TPR@0.1% FPR compared to the original (in-distribution) audit set. In contrast, OOD canaries are much more vulnerable. We defer those and additional results to Appendix B.1 for brevity.

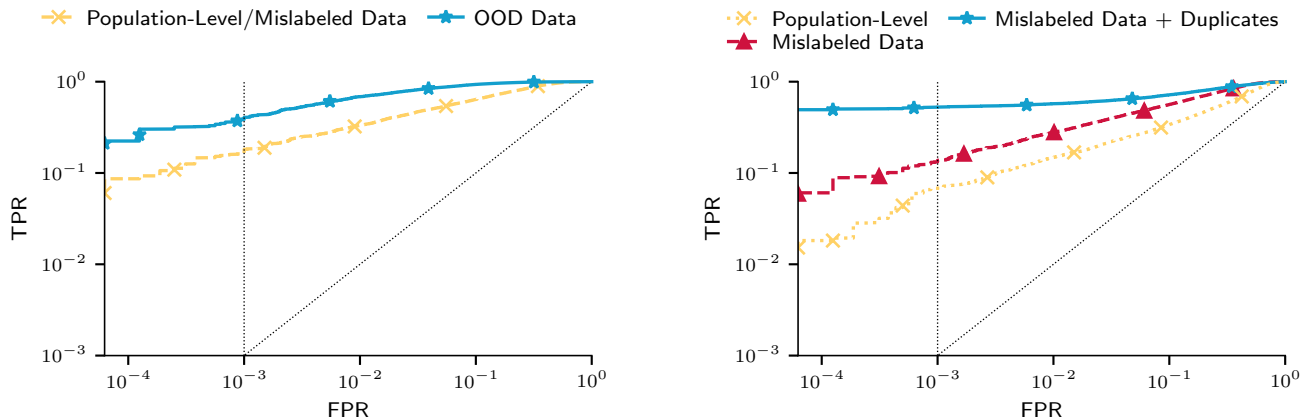
(Near)-duplicates are strong canaries for SELENA. Recall that SELENA first trains an ensemble of models f_1, \dots, f_K on overlapping subsets of the training data. SELENA then distills each sample x into a student model using only predictions from the teacher models that were *not* trained on x . Tang et al. [52] prove that SELENA’s ensemble mechanism leaks nothing about a sample’s membership if queried only on that specific sample.

Unfortunately, this proof ignores *interactions* between samples. Concretely, suppose that training a model on a mislabeled sample (x, \hat{y}) also affects the model’s prediction on a different training image x' , for example, because x' and x are similar. When SELENA distills x' into the student model, it will only query teachers f_i not trained on x' . However, some of these teachers will have been trained on the mislabeled sample (x, \hat{y}) . In that case, we expect that $f_i(x') \approx f_i(x) = \hat{y}$, that is, the incorrect label may *leak* into the student via predictions on other samples. We find evidence of this effect in practice: if we evaluate SELENA on mislabeled canaries, we get a TPR of 13.8% at 0.1% FPR, about twice as high as for the correctly labeled audit set.

Thus, SELENA might not protect some samples due to *other samples with similar features* in the training data (we investigate this more thoroughly in Appendix B.3). More precisely, we expect that the most vulnerable samples for SELENA are mislabeled images (x, \hat{y}) for which a *near-duplicate* $x' \approx x$ also exists in the training set (x' may be correctly labeled).

Tang et al. [52, App. A.3] conjecture that such samples are unlikely to exist in practice. Yet, we find that CIFAR-10 does contain mislabeled/ambiguous samples with near-duplicates in the training data (see the examples in Figure 11 in Appendix B.3).

This inspires our canary choice: We duplicate half of the original audit set, and mislabel one sample per pair. We then use these 500 samples as the new audit set (i.e., we randomly include each of those samples as a member with 50% probability) but we only evaluate the attack on the mislabeled 250 instances. Figure 6b confirms our hypothesis: attacks on mislabeled samples with duplicates in the audit set achieve a TPR of 52.7% at 0.1% FPR—a roughly 3.8× increase compared to mislabeled samples in isolation.



(a) *OOD samples are strong canaries for SSL defenses.* For SimCLR, using our adaptive white-box attack, OOD ImageNet data (blue) is more vulnerable to membership inference than the population average (yellow). Note that neither the SSL encoder nor our white-box attack depend on labels; hence, mislabeling an audit sample does not change its privacy leakage. See Appendix B.1 for more details and the MoCo-based defense.

(b) *(Near)-duplicates in the training data create particularly vulnerable samples for SELENA.* Mislabeled canaries in isolation (red) only mildly increase privacy leakage over a population-level evaluation (yellow). However, those mislabeled samples become highly vulnerable if they have a duplicate in the training set (blue).

Figure 6: The right choice of canary set reveals privacy leakage that is much higher than when the attack success is aggregated over the entire dataset. Different defenses require different canaries. While mislabeled samples are often a reasonable choice, we find that (a) OOD data for SSL and (b) mislabeled *duplicated* samples for SELENA are particularly vulnerable.

Note that the TPR is just above 50%, even at very low FPRs. This is because the attack succeeds when the mislabeled sample (x, \hat{y}) is a member, *conditioned on the near-duplicate x' also being a member*. Since we vary membership of all audit samples independently at random, this happens with probability 50%—bounding the expected number of successes. In Appendix B.3, we consider a stronger setting, where the near-duplicates are always part of the training data; we find that this enables near-perfect membership inference.

5.5 Strong DP-SGD Baselines

As we have shown, none of the heuristic defenses we study provides reasonable privacy protection for the most vulnerable samples. We hence ask whether this indicates that such leakage is inherent for a high-accuracy model trained on CIFAR-10, or if other heuristic defenses could provide a better tradeoff.

We consider DP-SGD [1] as a natural baseline to answer this question. However, for a fair comparison with other heuristic defenses, we focus on a high-utility regime; that is, we view DP-SGD as a purely heuristic defense while possibly forgoing meaningful provable guarantees. Concretely, we consider two DP-SGD instances: a medium utility baseline that maximizes empirical privacy constrained to at least 88% CIFAR-10 test accuracy, and a high utility baseline with 91% test accuracy. We show that high-utility DP-SGD yields a very competitive privacy-utility tradeoff, surpassing all the other heuristic defenses we consider (at a similar utility level).

DP-SGD baselines. Both baselines rely on state-of-the-art DP-SGD training techniques [14, 47]. We use a modified WRN16-4 architecture that replaces batch normalization with group normalization, swaps the order of normalization and ReLU, and uses the custom initialization scheme of [14]. We further employ augmentation multiplicity [14] using the modified Opacus [66] library of

Sander et al. [47], and return an exponential moving average of the model weights with decay factor 0.9999.

We tune the hyperparameters of the medium utility baseline in the same way as for all case studies (see Section 5.2), that is, to maximize privacy (measured by ϵ at $\delta = 10^{-5}$) subject to at least 88% CIFAR-10 test accuracy. Crucially, we do *not* enforce meaningful DP guarantees; the provable privacy guarantees ϵ of all our DP-SGD baselines are in the thousands. For the high utility baseline, we rely on recent scaling laws [47] to increase the medium baseline’s utility at the cost of privacy (primarily by decreasing batch size while carefully scaling noise). See Table 3 for all hyperparameters, and the average CIFAR-10 test accuracy over 64 models.

Adaptive attacks and canaries for DP-SGD. We consider the same threat model as in our case studies, in contrast to typical DP-SGD audits, where adversaries can observe and influence all model updates [41].

As canaries, we consider three types of outlier data that have been used for DP-SGD auditing in prior work [38, 41, 50]: mislabeled samples, OOD data, and uniform images. We explicitly omit adversarial examples (as used in [41]), since auditing many of these samples in parallel induces a weak (non-adaptive) form of adversarial training [55]. This would cause each individual canary to be less effective, as the partially robust model would be more likely to correctly classify the canaries that are *not* in the training set.

For attacks, we consider the same setting as for other defenses, where the attacker only gets access to the final model after training. In the DP-SGD literature, this is often called a black-box attacker, as opposed to a white-box attacker who can see each noisy gradient step. In this threat model, there are (to the best of our knowledge) no known adaptive attacks on DP-SGD that outperform standard

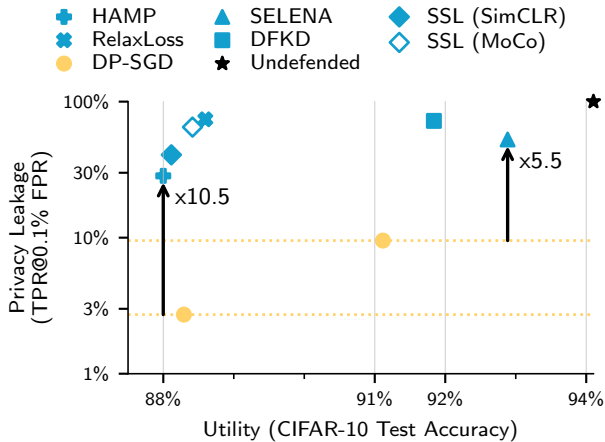


Figure 7: DP-SGD is a strong empirical privacy defense. We compare the privacy-utility tradeoff of the 5 heuristic defenses we study to two DP-SGD baselines tuned for high test accuracy. For both baselines, the DP-SGD privacy analysis yields near-vacuous guarantees ($\epsilon \gg 1,000$), yet both provide much better empirical privacy for the most vulnerable samples, according to our evaluation.

attacks like LiRA. We thus use LiRA on the final trained model, but report the maximum TPR@0.1% FPR over all canary types.

Results. Figure 7 compares the heuristic defenses we consider to our DP-SGD baselines (all evaluated according to our protocol, with adaptive attacks and strong canaries). Despite meaningless provable guarantees ($\epsilon > 10^8$), our high utility DP-SGD baseline shows decent empirical privacy: all heuristic defenses with similar test accuracy yield a TPR@0.1% FPR that is at least 5.5 \times worse. Compared to the medium utility DP-SGD baseline ($\epsilon > 3,000$), even the most private heuristic defense we study (HAMP) leaks 10 \times more membership privacy, at a slightly worse test accuracy.

Two defenses in our case studies (DFKD and SELENA) achieve slightly higher utility than our best DP-SGD baseline ($\approx 92\text{--}93\%$ CIFAR-10 test accuracy)—albeit at the cost of much higher privacy leakage. This raises the question if *any* defense can provide meaningful membership privacy for the most vulnerable samples in this very high utility regime (without using public data). There is evidence to suggest that the answer may be negative. In particular, the work of Feldman [19] proves that classifiers trained on heavy-tailed data distributions necessarily need to memorize some training labels to achieve optimal generalization. Correctly classifying the tail of the CIFAR-10 test data might thus require memorization of similar rare examples during training, rendering those examples susceptible to membership inference. To give more credence to this hypothesis, Appendix B.4 shows that even DP-SGD fails to provide reasonable privacy when pushed to reach around 92% test accuracy.

Ultimately, we do not claim that DP-SGD is the best membership inference defense in all settings. Yet, we show how—even absent meaningful provable guarantees ($\epsilon \gg 1,000$)—DP-SGD is a strong *empirical* defense with competitive utility on CIFAR-10. Thus, future heuristic defenses that aim to claim a better privacy-utility tradeoff than DP-SGD should show a clear advantage over our baselines.

6 CONCLUSION

Throughout this paper, we have illustrated three major methodological pitfalls in empirical privacy evaluations using membership inference attacks. Existing evaluations report metrics that do not convey meaningful individual privacy semantics, use weak attacks, and consider subpar DP baselines. The evaluation methodology we propose is one way to fix these issues. Our work exposes a number of possible takeaways and future research directions.

Privacy semantics in-between average-case and worst-case.

As we show, the exact way we measure the privacy of a defense matters a lot. Before evaluating a defense—or an attack—we thus need to clearly define the privacy *semantics* that the evaluation targets (e.g., do we care about the proportion of samples that can be inferred, or if *any* sample can be inferred).

These privacy semantics are often implicit in the formal membership inference game that a work starts from (e.g., are the dataset and target sample chosen randomly or by the adversary?), but this is rarely explicitly discussed. Ultimately, these choices interpolate between an average-case setting—where the data and target are randomly chosen—and a worst-case setting—where the dataset and target are adversarial. The design of heuristic privacy defenses is often motivated by the fact that the latter worst-case setting is overly pessimistic. But this need not imply that the other extreme (the fully average-case setting) is appropriate either.

A theory of “natural” privacy leakage. A possibly surprising finding from our work is that “heuristic DP-SGD” (with hyperparameters that do not provide meaningful provable guarantees) is by far the best defense in practice. Yet, the DP-SGD analysis is tight in worst-case (possibly pathological) settings [1, 20, 41]. A formal understanding of DP-SGD’s performance in “natural” settings might thus lead to tighter provable privacy under realistic assumptions.

Another intriguing question raised by our work (and others [27, 41]) is how to create strong canaries for a given defense. That is, how do we design or efficiently identify samples that are most vulnerable to privacy attacks? In our setting, an additional goal is to design a *collection* of such samples, where each sample is independently highly vulnerable. For now, we rely primarily on heuristics to select such samples, rather than on a principled approach.

DP-SGD is a pragmatic defense. A welcome finding from our work is that DP-SGD may be the “best-in-class” defense to apply in practice, whether one cares about stringent provable privacy guarantees or not. As a result, a single infrastructure and set of tools can be used for cases where data privacy is paramount (by setting hyperparameters to get strong provable privacy), as well as for cases where absence of memorization is a “nice to have” (by setting hyperparameters to get high utility).

ACKNOWLEDGMENTS

M.A. and J.Z. are funded by the Swiss National Science Foundation (SNSF) project grant 214838. We thank Matthew Jagielski for providing us with the 20,000 CIFAR-10 models used in Figure 2.

REFERENCES

- [1] Martin Abadi, Andy Chu, Ian Goodfellow, H. Brendan McMahan, Ilya Mironov, Kunal Talwar, and Li Zhang. 2016. Deep Learning with Differential Privacy. In *ACM SIGSAC Conference on Computer and Communications Security*. ACM, 308–318.
- [2] Anish Athalye, Nicholas Carlini, and David Wagner. 2018. Obfuscated gradients give a false sense of security: Circumventing defenses to adversarial examples. In *International conference on machine learning*. PMLR, 274–283.
- [3] Martin Bertran, Shuai Tang, Michael Kearns, Jamie Morgenstern, Aaron Roth, and Zhiwei Steven Wu. 2023. Scalable Membership Inference Attacks via Quantile Regression. In *Advances in Neural Information Processing Systems*.
- [4] Nicholas Carlini, Steve Chien, Milad Nasr, Shuang Song, Andreas Terzis, and Florian Tramer. 2022. Membership inference attacks from first principles. In *2022 IEEE Symposium on Security and Privacy (SP)*. IEEE, 1897–1914.
- [5] Nicholas Carlini, Vitaly Feldman, and Milad Nasr. 2022. No Free Lunch in Privacy for Free: How does Dataset Condensation Help Privacy?. *arXiv preprint arXiv:2209.14987* (2022).
- [6] Nicholas Carlini, Matthew Jagielski, Chiyuan Zhang, Nicolas Papernot, Andreas Terzis, and Florian Tramer. 2022. The Privacy Onion Effect: Memorization Is Relative. In *Advances in Neural Information Processing Systems*. 13263–13276.
- [7] Nicholas Carlini, Chang Liu, Úlfar Erlingsson, Jernej Kos, and Dawn Song. 2019. The secret sharer: Evaluating and testing unintended memorization in neural networks. In *USENIX Security Symposium*. 267–284.
- [8] Nicholas Carlini, Florian Tramer, Eric Wallace, Matthew Jagielski, Ariel Herbert-Voss, Katherine Lee, Adam Roberts, Tom Brown, Dawn Song, Úlfar Erlingsson, et al. 2021. Extracting training data from large language models. In *USENIX Security Symposium*.
- [9] Dingfan Chen, Ning Yu, and Mario Fritz. 2022. RelaxLoss: Defending Membership Inference Attacks without Losing Utility. In *International Conference on Learning Representations*.
- [10] Hanting Chen, Yunhe Wang, Chang Xu, Zhaohui Yang, Chuanjian Liu, Boxin Shi, Chunjing Xu, Chao Xu, and Qi Tian. 2019. Data-free learning of student networks. In *Proceedings of the IEEE/CVF international conference on computer vision*. 3514–3522.
- [11] Ting Chen, Simon Kornblith, Mohammad Norouzi, and Geoffrey Hinton. 2020. A simple framework for contrastive learning of visual representations. In *International conference on machine learning*. 1597–1607.
- [12] Zitao Chen and Karthik Pattabiraman. 2024. Overconfidence Is a Dangerous Thing: Mitigating Membership Inference Attacks by Enforcing Less Confident Prediction. In *NDSS Symposium*.
- [13] Christopher A Choquette-Choo, Florian Tramer, Nicholas Carlini, and Nicolas Papernot. 2021. Label-only membership inference attacks. In *International Conference on Machine Learning*. PMLR, 1964–1974.
- [14] Soham De, Leonard Berrada, Jamie Hayes, Samuel L Smith, and Borja Balle. 2022. Unlocking high-accuracy differentially private image classification through scale. *arXiv preprint arXiv:2204.13650* (2022).
- [15] Damien Desfontaines. 2021. A list of real-world uses of differential privacy. <https://desfontain.es/privacy/real-world-differential-privacy.html>. Ted is writing things (personal blog).
- [16] Tian Dong, Bo Zhao, and Lingjuan Lyu. 2022. Privacy for free: How does dataset condensation help privacy?. In *International Conference on Machine Learning*. PMLR, 5378–5396.
- [17] Cynthia Dwork, Frank McSherry, Kobbi Nissim, and Adam Smith. 2006. Calibrating noise to sensitivity in private data analysis. In *Theory of Cryptography: Third Theory of Cryptography Conference, TCC 2006, New York, NY, USA, March 4-7, 2006. Proceedings 3*. Springer, 265–284.
- [18] Gongfan Fang, Kanya Mo, Xinchao Wang, Jie Song, Shitao Bei, Haofei Zhang, and Mingli Song. 2022. Up to 100x faster data-free knowledge distillation. In *Proceedings of the AAAI Conference on Artificial Intelligence*, Vol. 36. 6597–6604.
- [19] Vitaly Feldman. 2020. Does learning require memorization? A short tale about a long tail. In *ACM SIGACT Symposium on Theory of Computing*. 954–959.
- [20] Shanglun Feng and Florian Tramèr. 2024. Privacy Backdoors: Stealing Data with Corrupted Pretrained Models. *arXiv preprint arXiv:2404.00473* (2024).
- [21] Matt Fredrikson, Somesh Jha, and Thomas Ristenpart. 2015. Model inversion attacks that exploit confidence information and basic countermeasures. In *ACM SIGSAC Conference on Computer and Communications Security*. 1322–1333.
- [22] Zhiwei Hao, Yong Luo, Han Hu, Jianping An, and Yonggang Wen. 2021. Data-free ensemble knowledge distillation for privacy-conscious multimedia model compression. In *Proceedings of the 29th ACM International Conference on Multimedia*. 1803–1811.
- [23] Kaiming He, Haoqi Fan, Yuxin Wu, Saining Xie, and Ross Girshick. 2020. Momentum contrast for unsupervised visual representation learning. In *Proceedings of the IEEE/CVF conference on computer vision and pattern recognition*. 9729–9738.
- [24] Kaiming He, Xiangyu Zhang, Shaoqing Ren, and Jian Sun. 2016. Deep Residual Learning for Image Recognition. In *IEEE Conference on Computer Vision and Pattern Recognition (CVPR)*. 770–778.
- [25] Xinlei He and Yang Zhang. 2021. Quantifying and mitigating privacy risks of contrastive learning. In *Proceedings of the 2021 ACM SIGSAC Conference on Computer and Communications Security*. 845–863.
- [26] Matthew Jagielski, Om Thakkar, Florian Tramer, Daphne Ippolito, Katherine Lee, Nicholas Carlini, Eric Wallace, Shuang Song, Abhradeep Guha Thakurta, Nicolas Papernot, and Chiyuan Zhang. 2022. Measuring Forgetting of Memorized Training Examples. In *The Eleventh International Conference on Learning Representations*.
- [27] Matthew Jagielski, Jonathan Ullman, and Alina Oprea. 2020. Auditing differentially private machine learning: How private is private sgd? *Advances in Neural Information Processing Systems* 33 (2020), 22205–22216.
- [28] Jinyuan Jia, Ahmed Salem, Michael Backes, Yang Zhang, and Neil Zhenqiang Gong. 2019. MemGuard: Defending against Black-Box Membership Inference Attacks via Adversarial Examples. In *ACM SIGSAC Conference on Computer and Communications Security*. 259–274.
- [29] Peter Kairouz, Sewoong Oh, and Pramod Viswanath. 2015. The composition theorem for differential privacy. In *International conference on machine learning*. PMLR, 1376–1385.
- [30] Myeongseob Ko, Ming Jin, Chenguang Wang, and Ruoxi Jia. 2023. Practical Membership Inference Attacks Against Large-Scale Multi-Modal Models: A Pilot Study. In *Proceedings of the IEEE/CVF International Conference on Computer Vision*. 4871–4881.
- [31] Alex Krizhevsky, Geoffrey Hinton, et al. 2009. Learning multiple layers of features from tiny images. (2009).
- [32] Hongbin Liu, Jinyuan Jia, Wenjie Qu, and Neil Zhenqiang Gong. 2021. EncoderMI: Membership inference against pre-trained encoders in contrastive learning. In *Proceedings of the 2021 ACM SIGSAC Conference on Computer and Communications Security*. 2081–2095.
- [33] Yugeng Liu, Rui Wen, Xinlei He, Ahmed Salem, Zhikun Zhang, Michael Backes, Emiliano De Cristofaro, Mario Fritz, and Yang Zhang. 2022. {ML-Doctor}: Holistic risk assessment of inference attacks against machine learning models. In *31st USENIX Security Symposium (USENIX Security 22)*. 4525–4542.
- [34] Yunhui Long, Lei Wang, Diyu Bu, Vincent Bindschaedler, Xiaofeng Wang, Haixu Tang, Carl A. Gunter, and Kai Chen. 2020. A Pragmatic Approach to Membership Inferences on Machine Learning Models. In *2020 IEEE European Symposium on Security and Privacy (EuroS&P)*. 521–534.
- [35] Raphael Gontijo Lopes, Stefano Fenu, and Thad Starner. 2017. Data-free knowledge distillation for deep neural networks. *arXiv preprint arXiv:1710.07535* (2017).
- [36] Aleksander Madry, Aleksandar Makelov, Ludwig Schmidt, Dimitris Tsipras, and Adrian Vladu. 2018. Towards Deep Learning Models Resistant to Adversarial Attacks. In *International Conference on Learning Representations*.
- [37] Nicolas M. Müller and Karla Markert. 2019. Identifying Mislabeled Instances in Classification Datasets. In *2019 International Joint Conference on Neural Networks (IJCNN)*. 1–8.
- [38] Milad Nasr, Jamie Hayes, Thomas Steinke, Borja Balle, Florian Tramèr, Matthew Jagielski, Nicholas Carlini, and Andreas Terzis. 2023. Tight Auditing of Differentially Private Machine Learning. In *USENIX Security Symposium*. 1631–1648.
- [39] Milad Nasr, Reza Shokri, and Amir Houmansadr. 2018. Machine learning with membership privacy using adversarial regularization. In *ACM SIGSAC Conference on Computer and Communications Security*. 634–646.
- [40] Milad Nasr, Reza Shokri, and Amir Houmansadr. 2019. Comprehensive privacy analysis of deep learning: Passive and active white-box inference attacks against centralized and federated learning. In *IEEE Symposium on Security and Privacy*. IEEE, 739–753.
- [41] Milad Nasr, Shuang Song, Abhradeep Thakurta, Nicolas Papernot, and Nicholas Carlini. 2021. Adversary instantiation: Lower bounds for differentially private machine learning. In *IEEE Symposium on Security and Privacy*. IEEE, 866–882.
- [42] Curtis G. Northcutt, Anish Athalye, and Jonas Mueller. 2021. Pervasive Label Errors in Test Sets Destabilize Machine Learning Benchmarks. In *Neural Information Processing Systems Datasets and Benchmarks Track*.
- [43] Nicolas Papernot, Martin Abadi, Úlfar Erlingsson, Ian Goodfellow, and Kunal Talwar. 2017. Semi-supervised Knowledge Transfer for Deep Learning from Private Training Data. In *International Conference on Learning Representations*. <https://openreview.net/forum?id=HkwSDPgg>
- [44] Francesco Pinto, Yaxi Hu, Fanny Yang, and Amartya Sanyal. 2024. PILLAR: How to Make Semi-Private Learning More Effective. In *2nd IEEE Conference on Secure and Trustworthy Machine Learning*.
- [45] Alexandre Sablayrolles, Matthijs Douze, Cordelia Schmid, Yann Ollivier, and Hervé Jégou. 2019. White-box vs black-box: Bayes optimal strategies for membership inference. In *International Conference on Machine Learning*. PMLR, 5558–5567.
- [46] Ahmed Salem, Yang Zhang, Mathias Humbert, Pascal Berrang, Mario Fritz, and Michael Backes. 2019. ML-Leaks: Model and Data Independent Membership Inference Attacks and Defenses on Machine Learning Models. (2 2019). <https://doi.org/10.60882/cispa.24612846.v1>
- [47] Tom Sander, Pierre Stock, and Alexandre Sablayrolles. 2023. TAN without a Burn: Scaling Laws of DP-SGD. In *Proceedings of the International Conference on*

- Machine Learning*, Vol. 202. 29937–29949.
- [48] Reza Shokri, Marco Stronati, Congzheng Song, and Vitaly Shmatikov. 2017. Membership inference attacks against machine learning models. In *IEEE Symposium on Security and Privacy*. IEEE, 3–18.
- [49] Adam D. Smith. 2020. Lectures 9 and 10. https://drive.google.com/file/d/1M_GfjSpEV2oaAuANKn2NJPYTDm1Mek0q/view.
- [50] Thomas Steinke, Milad Nasr, and Matthew Jagielski. 2023. Privacy Auditing with One (1) Training Run. In *Advances in Neural Information Processing Systems*. 49268–49280.
- [51] Thomas Steinke and Jonathan Ullman. 2020. The Pitfalls of Average-Case Differential Privacy. [DifferentialPrivacy.org](https://differentialprivacy.org/average-case-dp/). <https://differentialprivacy.org/average-case-dp/>.
- [52] Xinyu Tang, Saeed Mahloujifar, Liwei Song, Virat Shejwalkar, Milad Nasr, Amir Houmansadr, and Prateek Mittal. 2022. Mitigating Membership Inference Attacks by Self-Distillation Through a Novel Ensemble Architecture. In *USENIX Security Symposium*. 1433–1450.
- [53] Florian Tramèr and Dan Boneh. 2020. Differentially Private Learning Needs Better Features (or Much More Data). In *International Conference on Learning Representations*.
- [54] Florian Tramèr, Nicholas Carlini, Wieland Brendel, and Aleksander Madry. 2020. On adaptive attacks to adversarial example defenses. *Advances in neural information processing systems* 33 (2020), 1633–1645.
- [55] Florian Tramèr, Alexey Kurakin, Nicolas Papernot, Ian Goodfellow, Dan Boneh, and Patrick McDaniel. 2018. Ensemble Adversarial Training: Attacks and Defenses. In *International Conference on Learning Representations*.
- [56] Florian Tramèr, Reza Shokri, Ayrton San Joaquin, Hoang Le, Matthew Jagielski, Sanghyun Hong, and Nicholas Carlini. 2022. Truth Serum: Poisoning Machine Learning Models to Reveal Their Secrets. In *Proceedings of the 2022 ACM SIGSAC Conference on Computer and Communications Security*. 2779–2792.
- [57] Florian Tramèr, Andreas Terzis, Thomas Steinke, Shuang Song, Matthew Jagielski, and Nicholas Carlini. 2022. Debugging differential privacy: A case study for privacy auditing. *arXiv preprint arXiv:2202.12219* (2022).
- [58] Wenhao Wang, Muhammad Ahmad Kaleem, Adam Dziedzic, Michael Backes, Nicolas Papernot, and Franziska Boenisch. 2024. Memorization in Self-Supervised Learning Improves Downstream Generalization. In *The Twelfth International Conference on Learning Representations*.
- [59] Lauren Watson, Chuan Guo, Graham Cormode, and Alexandre Sablayrolles. 2021. On the Importance of Difficulty Calibration in Membership Inference Attacks. In *International Conference on Learning Representations*.
- [60] Yuxin Wen, Arpit Bansal, Hamid Kazemi, Eitan Borgnia, Micah Goldblum, Jonas Geiping, and Tom Goldstein. 2022. Canary in a Coalmine: Better Membership Inference with Ensembled Adversarial Queries. In *The Eleventh International Conference on Learning Representations*.
- [61] Ziqi Yang, Bin Shao, Bohan Xuan, Ee-Chien Chang, and Fan Zhang. 2020. Defending Model Inversion and Membership Inference Attacks via Prediction Purification. *arXiv:2005.03915 [cs.CR]*
- [62] Jiayuan Ye, Anastasia Borovykh, Soufiane Hayou, and Reza Shokri. 2023. Leave-One-out Distinguishability in Machine Learning. In *International Conference on Learning Representations*.
- [63] Jiayuan Ye, Aadyaa Maddi, Sasi Kumar Murakonda, Vincent Bindschaedler, and Reza Shokri. 2022. Enhanced membership inference attacks against machine learning models. In *Proceedings of the 2022 ACM SIGSAC Conference on Computer and Communications Security*. 3093–3106.
- [64] Samuel Yeom, Irene Giacomelli, Matt Fredrikson, and Somesh Jha. 2018. Privacy risk in machine learning: Analyzing the connection to overfitting. In *2018 IEEE 31st computer security foundations symposium (CSF)*. IEEE, 268–282.
- [65] Hongxu Yin, Pavlo Molchanov, Jose M Alvarez, Zhizhong Li, Arun Mallya, Derek Hoiem, Niraj K Jha, and Jan Kautz. 2020. Dreaming to distill: Data-free knowledge transfer via deepinversion. In *Proceedings of the IEEE/CVF Conference on Computer Vision and Pattern Recognition*. 8715–8724.
- [66] Ashkan Yousefpour, Igor Shilov, Alexandre Sablayrolles, Davide Testuggine, Karthik Prasad, Mani Malek, John Nguyen, Sayan Ghosh, Akash Bharadwaj, Jessica Zhao, Graham Cormode, and Ilya Mironov. 2021. Opacus: User-Friendly Differential Privacy Library in PyTorch. *arXiv preprint arXiv:2109.12298* (2021).
- [67] Sergey Zagoruyko and Nikos Komodakis. 2016. Wide Residual Networks. In *BMVC*.
- [68] Sajjad Zarifzadeh, Philippe Liu, and Reza Shokri. 2024. Low-Cost High-Power Membership Inference Attacks. *arXiv:2312.03262 [cs, stat]*
- [69] Jie Zhang, Chen Chen, Bo Li, Lingjuan Lyu, Shuang Wu, Shouhong Ding, Chunhua Shen, and Chao Wu. 2022. Dense: Data-free one-shot federated learning. *Advances in Neural Information Processing Systems* 35 (2022), 21414–21428.
- [70] Jie Zhang, Chen Chen, and Lingjuan Lyu. 2023. IDEAL: Query-Efficient Data-Free Learning from Black-Box Models. In *The Eleventh International Conference on Learning Representations*. <https://openreview.net/forum?id=ConT6H7MWL>
- [71] Xinbin Zhang. 2017. An Improved Method of Identifying Mislabelled Data and the Mislabelled Data in MNIST and CIFAR-10.

A EXPERIMENTAL DETAILS

A.1 Experimental Details in Figure 1

Figure 1 compares typical evaluations of membership privacy defenses to our proposed protocol. The bars labeled “Original” indicate the TPR@0.1% FPR of LiRA on a population-level, while “Ours” corresponds to a sample-level evaluation using adaptive attacks (see Section 5.3) and strong canaries (see Table 2). We otherwise use the same experimental setup as in the rest of this paper; see Section 5.2 for details.

For brevity, we only display the high utility DP-SGD baseline, and skip the medium utility baseline (which is more private). Similarly, for SSL, we only show the results from a white-box attack on SimCLR, and omit the (stronger) results for MoCo (see Figure 10c).

We list the full TPR@0.1% FPR values and test accuracy in Table 1 for completeness. Note that our canary choices and our audit setup only marginally affect test accuracy, but uncover significantly higher privacy leakage.

A.2 Experimental Details in Figure 2

The experiments in Figure 2 use 20,000 shadow models trained on CIFAR-10 without any defense. Each model randomly includes or excludes every CIFAR-10 sample in its training data such that each sample is a member in exactly half (10,000) of the models.

To obtain comparable results for population-level and sample-level evaluations, we first randomly select 64 models as shadow models, and use the remaining 19,936 as victim models.

For every CIFAR-10 sample x , we then use the 64 shadow models as in the standard LiRA attack to calculate member and non-member score distributions $\mathcal{N}(\mu_{x,\text{in}}, \sigma_{x,\text{in}}^2)$ and $\mathcal{N}(\mu_{x,\text{out}}, \sigma_{x,\text{out}}^2)$, respectively, and obtain test scores $\mathcal{A}(f, x)$ for every victim model f . The only difference between the population-level and sample-level metrics is how we aggregate those test scores.

Population-level. For the population-level evaluation in Figure 2a, we calculate an ROC curve over test scores $\mathcal{A}(f, \cdot)$ for each victim model f individually. This hence results in 19,936 population-level ROC curves, each over 50,000 test scores per victim f . We then determine the TPR@0.1% FPR for each individual per-model ROC curve, and report the average over all victim models. This corresponds to 19,936 population-level evaluations as done in previous work; we report the mean to control for randomness in different victim models.

Sample-level. For sample-level evaluations, we instead calculate a ROC curve for each sample x individually, aggregating the test scores $\mathcal{A}(\cdot, x)$ from all 19,936 victim models. This hence results in 50,000 sample-level ROC curves, each based on 19,936 test scores. We report the TPR@0.1% FPR for each sample’s curve in Figure 2a, and the full curve of the most vulnerable sample in Figure 2b.

Top-500 most vulnerable samples and 500 canaries. First, for the top-500 most vulnerable samples in Figure 2b, we determine the 500 samples with the highest sample-level TPR@0.1%, and aggregate their test scores on all victim models (resulting in an ROC curve over $500 \cdot 19,936$ test scores). Second, we use mislabeled samples as the 500 canaries in Figure 2b. We audit those canaries using the same setup as for all case studies in this work (see Section 5.2), but also randomly vary the membership of non-audit samples between

Table 1: Full privacy (TPR@0.1% FPR) and utility (CIFAR-10 test accuracy) values for each defense.

Method	TPR@0.1% FPR		CIFAR-10 Test Accuracy	
	Population-Level, LiRA	Sample-Level, Adaptive Attack	Population-Level	Sample-Level
HAMP	2.1%	28.5%	88.29% (± 0.04)	88.00% (± 0.04)
RelaxLoss	2.2%	74.1%	88.86% (± 0.03)	88.60% (± 0.03)
SELENA	6.8%	52.7%	93.05% (± 0.02)	92.88% (± 0.02)
SSL (SimCLR)	5.8%	40.6%	88.18% (± 0.02)	88.11% (± 0.03)
SSL (MoCo)	2.0%	65.0%	88.44% (± 0.04)	88.41% (± 0.04)
DFKD	1.3%	72.2%	92.39% (± 0.03)	91.84% (± 0.03)
DP-SGD (medium utility)	0.7%	2.7%	88.29% (± 0.03)	88.29% (± 0.03)
DP-SGD (high utility)	2.2%	9.5%	91.13% (± 0.03)	91.12% (± 0.02)
DP-SGD (very high utility)	4.8%	63.2%	91.89% (± 0.03)	91.79% (± 0.03)
Undefended	13.4%	100.0%	94.52% (± 0.02)	94.10% (± 0.02)

shadow models (i.e., include or exclude *every* CIFAR-10 sample in each shadow model such that every sample is in exactly half of the models’ training data) to yield a comparable setting.

A.3 Validation of Our Auditing Setup

The goal of our evaluation protocol is to mimic realistic model deployments. However, most existing evaluations vary the membership of all samples in a dataset. For CIFAR-10, this yields 25k training samples in expectation—underestimating utility, and likely increasing memorization. We hence use an approach similar to Steinke et al. [50]: audit only a small subset of the training data, and always include all other samples in the training data.

While our approach results in realistic models, it yields a stronger adversary that knows almost all training data. In the extreme case of a single audit sample, such an adversary might even reconstruct that sample’s features [62]. We thus verify that our approach yields ROC curves comparable to previous methodology.

As in our case studies, we train 64 models, and attack a small “audit” subset of CIFAR-10 using LiRA in a leave-one-out fashion. We compare the effects of varying and fixing the membership of non-audit samples as follows:

- (1) Varying membership: Resample the training set membership of all CIFAR-10 samples for each shadow model.
- (2) Fixed membership: Resample only the membership of audit samples between shadow models, and use the same fixed (random) membership for non-audit samples.

Note that both approaches yield an expected training set size of 25k samples; the only difference is whether non-audit samples are the same for different shadow models. Varying membership corresponds to most existing evaluations, while fixed membership mimics our procedure. For a full picture, we consider both 500 audit samples as in our case studies, and audit sets of size 250, proportional to half of CIFAR-10.

The results in Figure 8 show that using the same non-audit samples in all shadow models (dashed lines) has mild effects. While the TPR@0.1% FPR minimally increases compared to varying the membership of all 50k samples in every shadow model (solid lines), the difference is negligible compared to the effects of different attacks or canaries. Considering the setting in our case studies (dotted

line), i.e., including all 49.5k non-audit CIFAR-10 samples in the training data of all shadow models, we find that the corresponding ROC curve matches or lies below all four other settings. Hence, our evaluation protocol allows us to judge a defense’s real-world privacy-utility tradeoff without inflating privacy leakage.

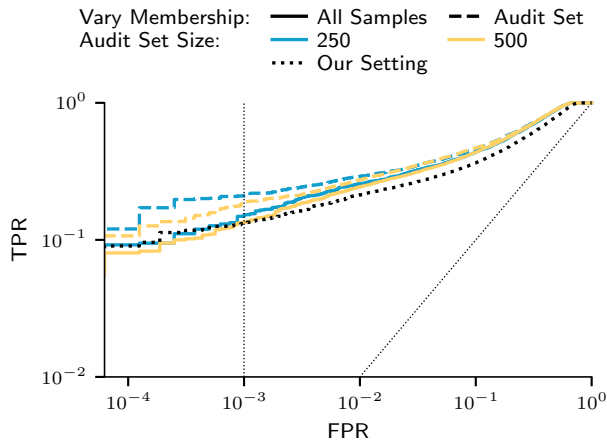


Figure 8: Our threat model yields comparable privacy estimates to prior work. Recall that prior work trains shadow models by randomly sampling the membership of each dataset point. In contrast, we only sample the images that we audit, and keep the remaining parts of the training set fixed. While this gives the attacker more power than in prior evaluations (i.e., the attacker knows a large fraction of the target model’s training set), we show this has a negligible effect on evaluation outcomes. For audit sets of size either 250 or 500, we compare the setting where we resample each image (solid lines) or where we only resample the audit set (dashed lines) and keep $\approx 25,000$ images fixed (to ensure training sets of similar sizes in both settings). Our audit setting (dotted line) just samples the audit set, and always uses the remaining CIFAR-10 training data (49,500 images) to train all shadow models. Our approach never overestimates privacy leakage.

A.4 Defense-Specific Hyperparameters and Implementation Details

HAMP. We tune the two hyperparameters that directly control the privacy-utility tradeoff (entropy threshold and regularization strength), and otherwise use the same hyperparameters as the original paper [12], including the same optimizer, learning rate schedule, number of training epochs, and not using data augmentation. As the set of potential privacy hyperparameters in [12] yields sub-par privacy in our setting, we consider a logarithmic grid of stronger values: entropy thresholds in $[0.684, 0.9999]$ and regularization strengths in $[0.001, 5.0]$. From the Pareto-optimal set, we fix the largest regularization strength that yields stable results, and pick the largest entropy threshold, subject to 88% test accuracy. This results in a regularization strength of 0.005 and an entropy threshold of 0.9996837722339832. For our simple label-only attack, we do *not* tune the ridge regularization strength of the logistic regression classifiers (because tuning would require us to train a separate set of shadow models), and use a default value of 1.0 instead. However, we find that even tuning the ridge regularization strength directly on the victim models does not significantly affect the TPR@0.1% FPR; see Appendix B.2.

RelaxLoss. As for HAMP, we tune the loss threshold (as it directly controls the privacy-utility tradeoff), but otherwise use the same hyperparameters as the original paper [9]. In particular, we also omit data augmentation, and restrict posterior flattening only to misclassified samples; we resolve ambiguities in the original paper by following the authors’ implementation.⁸ To find the optimal loss threshold in our setting, we search a logarithmic grid of values in $[0.0100, 2.1813]$, and pick the largest threshold that yields at least 88% CIFAR-10 test accuracy; this yields a loss threshold of 0.5946.

SELENA. Since it is unclear how the number of queries and ensemble members affect privacy, we use the values proposed by SELENA’s authors, that is, performing 10 queries over 25 models. We further use the same training procedure and hyperparameters as the original paper [52].

SSL. For both SimCLR and MoCo, we train an encoder with feature dimension 128 for 800 epochs, and then fit a linear classifier for an additional 100 epochs while fixing the encoder. Encoder training, uses a batch size of 512, momentum 0.9, weight decay 0.0005, and a learning rate of 0.06. For the linear classifier, we use a cross-entropy loss, a learning rate of 0.5 and batch size 256. MoCo additionally relies on a queue during training, we set the size to 4096.

DFKD. Following the setting in [18], we find that only using the “BN” loss (i.e., matching the batch-normalization statistics of the teacher model, widely used in many DFKD methods) yields a sufficiently high accuracy of at least 88%. Therefore, for the sake of simplicity, we only employ that loss for the generation of synthetic data. This approach facilitates the generalization of our evaluation to numerous other DFKD methods. Apart from that, we perform for 240 iterations: In each iteration, we first generate 256 new images, obtain teacher model predictions, and store the result into a “memory bank”. We then train the student model for 5 epochs on the full memory bank.

⁸<https://github.com/DingfanChen/RelaxLoss/>

Undefended. For the undefended baseline in Figure 7, we aim to mimic the hyperparameters of defenses in our case studies. Concretely, we train WRN16-4 models using SGD with momentum 0.9 and weight decay 0.0005, batch size 256, and typical data augmentation (random horizontal flips and shifts of up to 4 pixels). We optimize for 200 epochs with a base learning rate of 0.1; we linearly warm up the learning rate during the first epoch, and then decay the learning rate with a factor of 0.2 at epochs 60, 120, and 160.

A.5 Canaries

Table 2 summarizes the adaptive canaries that we use to audit each defense in our study.

Table 2: Canaries have to be adapted to the defense. Mislabeled samples are powerful canaries for most defenses that rely on a standard supervised learning paradigm, but fail to reliably mimic the leakage of the most vulnerable samples for SELENA or SSL.

Method	Canary Choice
HAMP	mislabeled samples
RelaxLoss	mislabeled samples
SELENA	mislabeled duplicates
SSL (SimCLR and MoCo)	OOD data (ImageNet)
DFKD	mislabeled samples
DP-SGD	mislabeled samples, or OOD data (ImageNet), or uniform data

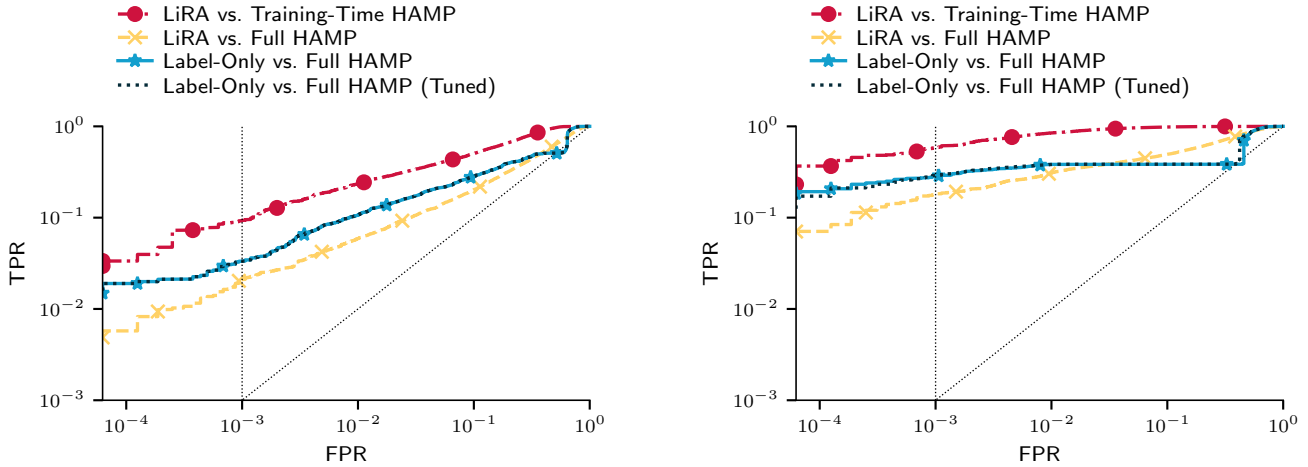
B ADDITIONAL EXPERIMENTS

B.1 Investigating Adaptive Attacks and OOD Effectiveness for SSL

In this section, we present the full results and additional details for both SimCLR and MoCo in white-box and black-box settings.

Adaptive attacks on a population level. Figure 10a shows the performance of our adaptive attack for MoCo on a population level (analogous to the SimCLR results in Figure 4a). We again find that using our adaptive score $\mathcal{S}(f; x)$ in LiRA mildly increases the TPR@0.1% FPR over standard confidence-based scores in a black-box setting (2.0% to 3.6%), and significantly in a white-box setting (to 23.6%, more than an 11x increase).

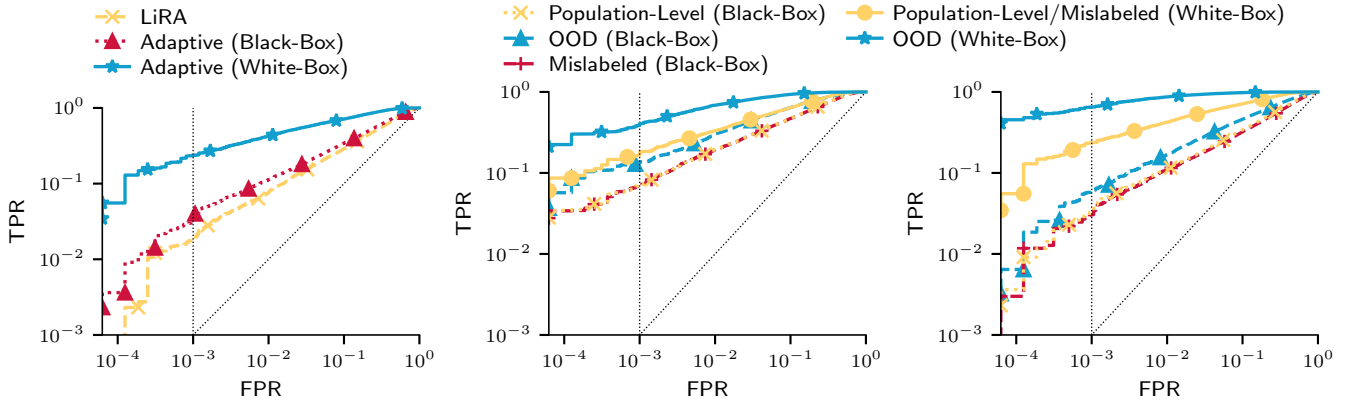
Adaptive attacks on OOD canaries. Figures 10b and 10c depict the full ROC curves of our adaptive attacks on both SSL defenses, comparing different types of canaries. Given that labels neither influence the SSL encoders nor our white-box attack, the ROC curves for mislabeled samples and the original audit set are identical in the white-box setting. Furthermore, in a black-box setting, mislabeled samples even yield slightly reduce TPR values. In contrast, we find that OOD data is a strong canary choice, since such outliers are significantly more vulnerable for both SSL methods and threat models.



(a) Full HAMP ROC curves on a *population-level* (original audit set).

(b) Full HAMP ROC curves on *mislabeled canaries*.

Figure 9: Full results for HAMP (a) across the dataset and (b) on mislabeled canaries. In both instances, HAMP’s training-time defense alone (red) does provide moderate privacy, but renders models highly private against LiRA when combined with the test-time defense (yellow). Yet, our simple label-only attack (blue) successfully circumvents the test-time defense. We further tune the hyperparameters of the label-only attack (black); this yields the default parameters for the population-level evaluation, and only marginally influences the ROC curve for the sample-level evaluation on mislabeled canaries.



(a) Our adaptive attack on the contrastive loss increases privacy leakage for models trained with MoCo, especially in the white-box setting.

(b) Full SimCLR ROC curves on OOD canaries.

(c) Full MoCo ROC curves on OOD canaries.

Figure 10: Additional SSL results. We show the attack success of our adaptive attack for MoCo on a population-level in (a), and the full ROC curves on OOD data for (b) SimCLR and (c) MoCo.

B.2 Full HAMP Results

As discussed in Section 5.3, HAMP’s test-time defense provides strong privacy against confidence-based attacks such as LiRA. The full population-level results in Figure 9a confirm that, while the training-time defense alone moderate protects privacy, the test-time defense reduces privacy leakage by an order of magnitude. Notably, LiRA achieves a $\text{TPR}@0.1\% \text{FPR}$ of only 2.1%—worse than against our high utility DP-SGD baseline! Yet, our simple label-only attack undoes part of that protection.

For mislabeled canaries, the differences are even more pronounced: as seen in Figure 9b, our label-only attack increases the $\text{TPR}@0.1\%$

FPR by over ten percentage points. Nevertheless, there is still over a $2\times$ difference between our label-only attack and LiRA directly targeting the training-time defense. We suspect that stronger (and more expensive) label-only attacks can close this gap.

Finally, note that in both cases, tuning the hyperparameters of our label-only attack only marginally influences the $\text{TPR}@0.1\% \text{FPR}$ compared to using default values; for population-level evaluations, the default and tuned hyperparameters even coincide.



Figure 11: Examples of near-duplicates with different labels in CIFAR-10. Our canary set for the SELENA defense mimics such samples. We highlight a selection of samples (top) and their nearest neighbors (bottom), where the two samples have different labels.

B.3 Disentangling Privacy Leakage of SELENA

Mislabeled near-duplicates in CIFAR-10. We base our canary choice on the intuition that certain mislabeled/ambiguous CIFAR-10 samples leak privacy through a near-duplicate in the training data. To show that such samples indeed exist, we calculate OpenCLIP embeddings⁹ of all CIFAR-10 samples, and use the pairwise cosine similarity to determine each sample’s nearest neighbor with a different label. We then inspect the pairs with the highest cosine similarity and plot a selection in Figure 11.

This process reveals multiple samples that match our hypothesis, many with correct labels, and some mislabeled. For example, we identify an image of a bird that closely resembles a different bird labeled “airplane”, or an image of a Sphynx cat that resembles a different image of a small dog. Since we use CLIP embeddings to identify those examples, we argue they are similar not only visually, but also in terms of neural network features. Further note that our goal is to identify the *most vulnerable sample* in CIFAR-10; hence, while the selection in Figure 11 is small, a single example suffices.

Investigating SELENA’s ensemble mechanism. SELENA’s first stage, called “Split-AI”, is the defense’s main privacy mechanism. Given an ensemble of models f_i and a query sample x , Split-AI aggregates predictions only from models not trained on x . Hence, in isolation, predictions on a training member and non-member should be similar. The second stage, distillation, serves to reduce computational cost during inference, and to avoid privacy leakage from certain Split-AI edge-cases. Yet, SELENA seems to leak more privacy of mislabeled samples than of the same data with original labels—even without explicit duplicates (see Figure 12b). We hence analyze Split-AI more thoroughly to better understand SELENA’s behavior on those samples.

Concretely, we consider two SELENA ensembles, one trained with the original 500 audit samples, and one with 500 mislabeled audit samples (but without adding duplicates). We then directly attack Split-AI in two ways: To obtain predictions on a target sample x , we either query Split-AI on x itself, or on its nearest neighbor (in the non-audit part of CIFAR-10). As before, we use the cosine similarity of OpenCLIP embeddings as a similarity metric, and

⁹https://github.com/mlfoundations/open_clip/, model ViT-S0400M-14-SigLIP-384 pretrained on the web1i dataset.

calculate a maximum-weight matching between audit and non-audit samples to ensure unique nearest neighbors.

The results in Figure 12a provide further evidence that near-duplicates are responsible for SELENA’s privacy leakage on mislabeled samples. If an attacker directly queries Split-AI on the audit samples, the resulting ROC curve is close to a random guessing baseline—even for mislabeled samples. However, if LiRA queries each audit sample’s nearest neighbor instead, the attack achieves a significantly higher TPR. Notably, the distillation stage of SELENA queries Split-AI on the full training set, including nearest neighbors of audit samples. Hence, the privacy leakage persists in the final student model, thus explaining the matching ROC curves on mislabeled canaries for attacks on Split-AI and the distilled student.

Stronger threat models. Attacking Split-AI on our canaries yields almost perfect membership inference (a TPR of 99.7% at 0.1% FPR, and 96.3% at 0% FPR), yet, attacking the distilled student on the same canaries reduces attack success by about half (52.7% TPR at 0.1% FPR). As argued in the main matter, we suspect that the cause is varying membership of near-duplicates. We hence consider a stronger threat model, where only the membership of canaries varies, and near-duplicates are in the training data of all models.

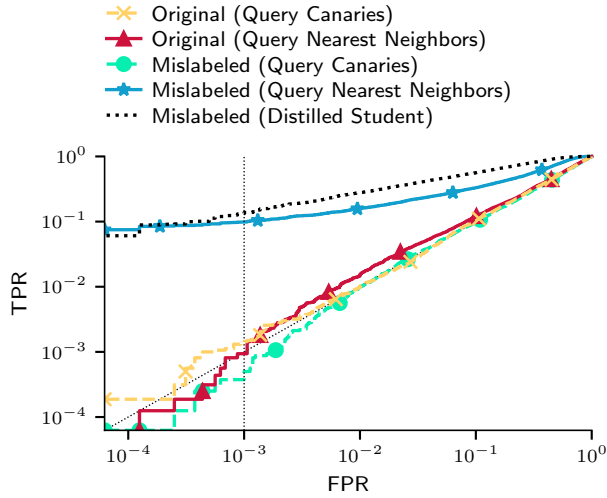
More concretely, we now mislabel *all* 500 original audit samples, create a copy of the full audit set (including the wrong labels), and append this copy to the training data of all models. As a baseline, we also consider the same procedure with a clean audit set; that is, we use the same 500 audit samples and copies, but all with the correct labels. The results in Figure 12b show that this stronger model is highly effective: if duplicates of mislabeled canaries are in the training data of all models, LiRA achieves an almost perfect TPR of 99.7% at 0.1% FPR (and 99% with zero false positives)—without explicitly exploiting the presence of duplicates.

While those results are impressive, the threat model is not entirely realistic. For one, we could not find any pairs of near-duplicate CIFAR-10 samples that are both mislabeled (neither with the same or different classes). What is more, the threat model resembles data poisoning; for example, the “Truth Serum” attack of Tramèr et al. [56] renders target samples more vulnerable to membership inference by inserting copies into the training data of a victim model.

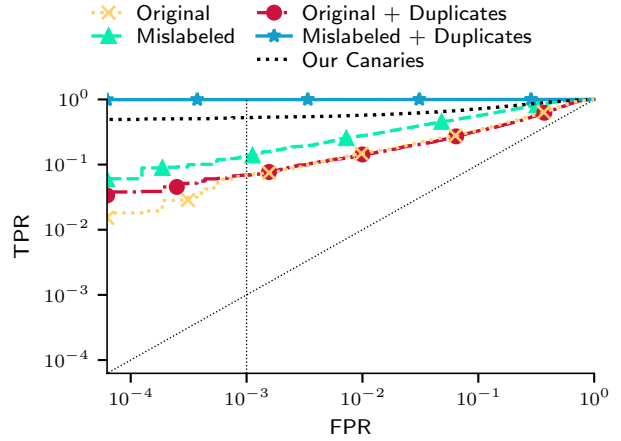
B.4 Pushing DP-SGD Utility

Given the strong empirical privacy of our medium and high utility DP-SGD baselines in Section 5.5, we ask if we can push DP-SGD’s accuracy even further, yet maintain reasonable privacy. We thus continue tuning the high utility baseline with the goal of reaching around 92% CIFAR-10 test accuracy.

However, as Table 3 shows, we are unable to achieve our goal. In particular, our best result raises the test accuracy by less than one percentage point (to 91.79%), yet exhibits a sample-level TPR@0.1% FPR of 63.2%. Notably, this is the first instance that one of our case studies (SELENA) yields stronger privacy at a higher utility than DP-SGD (even though, at over 50% TPR@0.1% FPR, both defenses are unsuitable for critical applications). Ultimately, it is likely that achieving very high utility while maintaining strong privacy is unachievable in practice, although a formal statement remains an open research question.



(a) Naturally occurring near-duplicates in CIFAR-10 render mislabeled samples more vulnerable for SELENA. We directly attack SELENA’s ensemble mechanism (Split-AI) on either original or mislabeled audit samples. If we directly query the audit samples, the attack never performs better than random guessing. However, if we attack a mislabeled sample (x, \hat{y}) by querying its nearest neighbor x' (the most similar image in the non-audit part of CIFAR-10), the resulting ROC curve is close to the one of the final distilled student.



(b) Including copies of mislabeled canaries in the training data completely breaks SELENA’s privacy. We compare SELENA evaluations using original and mislabeled audit samples, once as-is, and once by including a copy of the audit set in every model’s training data. The latter enables close-to-perfect membership inference, almost doubling the TPR@0.1% FPR compared to our proposed canaries—albeit in the stronger “privacy poisoning” threat model introduced in Tramèr et al. [56].

Figure 12: Additional results for privacy leakage in SELENA. In (a), we directly attack SELENA’s first defense stage (Split-AI), querying either target samples directly, or their nearest neighbor in the non-audit data. In (b), we consider a slightly stronger threat model, where mislabeled duplicates enable almost perfect membership inference—even on the full defense.

Table 3: Full details for DP-SGD baselines on CIFAR-10.

	Medium	High	Very High
Test accuracy	88.29% (± 0.03)	91.13% (± 0.03)	91.79% (± 0.03)
DP ϵ ($\delta = 10^{-5}$)	≈ 3558	$\approx 1.8 \cdot 10^8$	$\approx 1.1 \cdot 10^9$
Noise multiplier	0.2	0.00625	0.003125
Clipping norm	1	1	1
Batch size	2048	64	64
Training epochs	200	16	25
Learning rate	4	4	4
Augmult	8	8	8

B.5 Extended Version of Figure 3

In Figure 3, we show a subset of the most vulnerable CIFAR-10 samples (for standard training) to highlight different types of potential canaries. Figure 13 contains the full list of the 40 most vulnerable samples and their corresponding sample-level TPR@0.1% FPR.

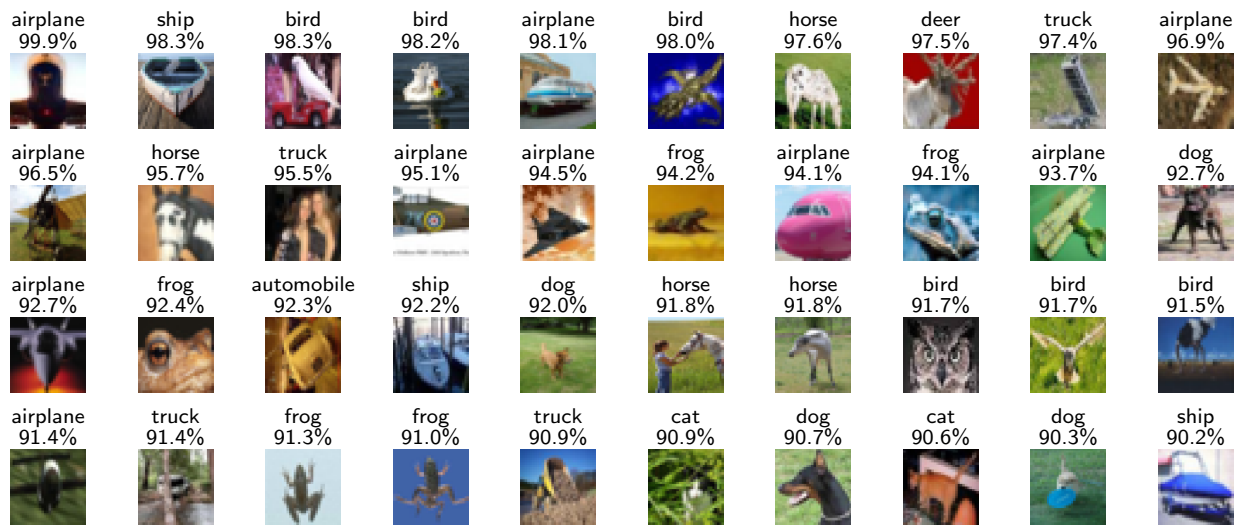


Figure 13: The 40 CIFAR-10 samples most vulnerable to membership inference, in the setting of Figure 2a. The samples are in order of decreasing privacy leakage. Titles above each image indicate the original label in CIFAR-10, and the sample-level $\text{TPR}@0.1\% \text{FPR}$.